Supplementary information for

High-rate and efficient ethylene electrosynthesis using a catalyst:promoter:transport layer

Adnan Ozden[1†], Fengwang Li[2†], F. Pelayo García de Arquer[2], Alonso Rosas-Hernández[3], Arnaud Thevenon[3], Yuhang Wang[2], Sung-Fu Hung[2], Xue Wang[2], Bin Chen[2], Jun Li[1,2], Joshua Wicks[2], Mingchuan Luo[2], Ziyun Wang[2], Theodor Agapie[3], Jonas C. Peters[3]*, Edward H. Sargent[2]* & David Sinton[1]**

[1]*Department of Mechanical and Industrial Engineering, University of Toronto, 5 King's College Road, Toronto, Ontario, M5S 3G8, Canada.*

[2]*Department of Electrical and Computer Engineering, University of Toronto, 10 King's College Road, Toronto, Ontario, M5S 3G4, Canada.*

[3]*Joint Center for Artificial Photosynthesis and Division of Chemistry and Chemical Engineering, California Institute of Technology, Pasadena, California, 91125, USA.*

[†]*These authors contributed equally to this work.*

**Correspondence and requests for materials should be addressed to David Sinton (D.S.) (sinton@mie.utoronto.ca), Edward H. Sargent (E.H.S.) (ted.sargent@utoronto.ca), Jonas C. Peters (J.C.P.) (jpeters@caltech.edu), and Theodor Agapie (T.A.) (agapie@caltech.edu).*

Tetrahydro-phenanthrolinium synthesis

N,N'-ethylene-phenanthrolinium dibromide molecular precursor was synthesized by following the procedure reported in our previous report.[1]

Materials characterization

Scanning electron microscopy (SEM) imaging and associated energy dispersive X-ray (EDX) elemental mapping were performed via a high-resolution scanning electron microscope (Hitachi S-5200). Cross-sectional SEM imaging was performed via Dual-beam FIB-SEM NB5000. X-ray photoelectron spectroscopy (XPS) measurements were carried out via PHI 5700 Electron Spectroscopy for Chemical Analysis (ESCA) system by using Al Kα X-ray radiation (1486.6 eV) as the energy source for excitation. Transmission electron microscopy (TEM) imaging was carried out via a field emission transmission electron microscope (Hitachi HF3300). XAS data were processed via the Athena software included in a standard IFEFFIT package. *In-situ* Raman measurements were performed by using a Renishaw inVia Raman Microscope equipped with a water immersion objective (63x, Leica Microsystems) and 785 nm laser. The *in-situ* Raman measurements were performed in a modified cell, in which an Ag/AgCl (3M KCl) reference electrode and a platinum (Pt) wire were employed as the reference and counter electrodes, respectively. The Raman spectra were obtained via the commercial software (Renishaw WiRE, version 4.4).

Electrode preparation

Copper target (Kurt J. Lesker Company) was evaporated onto a single side of the polytetrafluoroethylene (PTFE) substrate (450 μm average pore size) with the sputtering rate of 0.50 Å/sec under 10^{-6} Torr. The sputtered Cu thickness was varied between 100 nm and 200 nm,

with the thickness increments of 25 nm. The phenanthrolinium-derived film was electro-deposited from a 0.1 M $KHCO_3$ solution containing 10 mM N,N'-ethylene-phenanthrolinium dibromide. The electrodeposition was performed in a three-electrode setup, in which Cu/PTFE was used as the working electrode (5 cm^2 geometric active surface area), Ag/AgCl (3M KCl) as the reference electrode, and Pt sheet as the counter electrode. Cyclic voltammetry was applied to the Cu/PTFE electrode in the range of -0.6 V and -2.0 V, with a scanning rate of 50 mV s^{-1}. The tetrahydro-phenanthrolinium loading on the Cu/PTFE electrode was controlled by varying the number of cycles**.** The ionomer deposition was carried out by spray-coating a solution of 17 µl perfluorosulfonic acid ionomer (PFSA, Aquivion® D79-25BS) and 3 mL methanol onto the tetrahydro-phenanthrolinium modified Cu/PTFE electrode with the sample size of 18 cm^2. The 3D CTPI electrode was obtained by spray-coating a solution containing Cu nanoparticles (NPs, 25 nm average particle size, Sigma-Aldrich), N,N'-ethylene-phenanthrolinium dibromide, and methanol (Sigma-Aldrich) onto the Cu/PTFE electrodes. The nominal Cu NPs loading and Cu NPs-to-SSC ionomer weight ratio (wt%) were optimized, and the optimum values were determined to be 1.25 mg cm^{-2} and 22.0 wt%, respectively. The weight ratio of N,N'-ethylene-phenanthrolinium dibromide with respect to the Cu NPs loading was optimized to be 7.5 wt%. The catalyst inks were prepared by following three sequential steps: (i) ultrasonically mixing Cu NPs with N,N'-ethylene-phenanthrolinium dibromide in 3 mL methanol for 30 min, (ii) incorporating 1 mL methanol solution containing the respective amount of ionomer into the resulting catalyst solution, and (iii) ultrasonically mixing the final Cu NPs: tetrahydro-phenanthrolinium:SSC ionomer containing slurry for 30 min.

Electrochemical performance and product analysis

The CO_2RR/CORR performance characteristics of the catalysts were investigated using an electrochemical test station. The experimental setup consisted of a potentiostat and a current booster (Metrohm Autolab, 10A), commercial CO_2RR membrane electrode assembly (MEA) electrolyzer (Dioxide Materials), mass flow controller (Sierra, SmartTrak 100), humidifier, peristaltic pump with silicon tubing, and anolyte container.

The main constituents of the CO_2 electrolyzer are MEA, anode and cathode flow fields (made of titanium and stainless steel, respectively), and anode and cathode conductive plates. The geometric active areas of both the anode and cathode flow fields were 5 cm^2. The MEA was comprised of cathode electrode, anode electrode (Ti-IrO_2 mesh), and anion exchange membrane (AEM, Sustainion® X37-50). The MEA was first placed between the anode and cathode flow fields and then assembled together through equally applied compression torque to the associated bolts. The flow fields were mainly responsible for effective supply of aqueous anolyte solution (0.1 M $KHCO_3$) and humidified CO_2 over the respective surfaces of anode and cathode electrodes. The anode and cathode gaskets were placed between the flow fields and respective electrodes to ensure sealing during reaction. To ensure good electrical contact between the cathode flow field and cathode electrode (Cu/PTFE), the cathode electrode was attached to the well cleaned stainless steel surface of the flow field by using a copper tape frame, which was then fully covered with a Kapton tape frame to eliminate copper tape's potential impact on reaction. The anode electrode (Ti-IrO_2) manufacturing involved several sequential steps: etching the Ti screens (Fuel Cell Store) in 6 M hydrochloric acid (HCl) solution for 40 min at 80°C, washing the etched Ti screens with deionized water (DI) to remove any potential impurities, immersing the Ti screens into a solution composed of isopropanol, iridium (IV) oxide dehydrate (Premion®,

99.99%, metals basis, Ir 73% min, Alfa Easer), and HCl, and drying (at 100°C for 10 min) and sintering (at 500°C for 10 min) to achieve the final form of titanium iridium oxide (Ti-IrO_2). These steps were repeated until the final Ir loading of 2 mg/cm^2 was achieved. The AEM was activated in a 1M KOH solution for over 24 h and immersed into water for 5 min prior to being mounted between the anode and cathode electrodes.

After the electrolyzer assembly, 0.1 M $KHCO_3$ was circulated through the anode side of the electrolyzer with the constant flow rate of 10 mL/min via a peristaltic pump, while the fully humidified CO_2 was supplied to the cathode side with the constant flow rate of 80 standard cubic centimeters per minute (SCCM) via the mass flow controller. After three-minutes of initial operation, the full cell potential of -3.0 V was applied to the electrolyzer, and then the potential was gradually increased from -3.0 V with the increments of -0.10 V. The voltage increments were made upon complete stabilization of the corresponding current, typically required 15-20 min. The current data for each corresponding potential were recorded while simultaneously collecting the CO_2RR gas products in 1 mL volume by using gas tight syringes (Hamilton chromatography syringe). For each applied potential, gas products were collected at least 3 times with proper time intervals. The gas samples were then injected into the gas chromatography (GC, PerkinElmer Clarus 680). The GC used for the gas product analysis comprises of three constituents: a flame ionization detector (FID), a thermal conductivity detector (TCD), and packed columns. The spectra obtained from the GC for each gas injection was utilized to calculate the FE towards gas products of CO_2RR/CORR.

For the stability test, the MEA electrolyzer was operated at a constant current density of 220 mA cm^{-2} by co-feeding CO_2 and N_2 with the constant stoichiometric ratio of 40%:60%. The gas products were collected at frequent time intervals, and for each data point, three continuous

injections were made, and thus each selectivity value in the stability curve was the average of three sequentially obtained FE values.

Faradaic efficiency (FE) calculations

FE towards any of CO_2RR gas products was calculated via Equation (2):

$$FE = \frac{i_a}{i_{total}} = \frac{n_a v_{CO_2} c_a F}{i_{total} V_m} \qquad \text{Equation (2)}$$

where i_a is the partial current of product α, i_{total} is the total current, n_a is the number of electrons that transfer to form 1 mol of product α, v_{CO_2} is the flow rate of CO_2 at the cell outlet, c_a is the concentration of product α measured via gas chromatography, F is the Faraday constant, and V_m is the unit molar volume under room conditions.

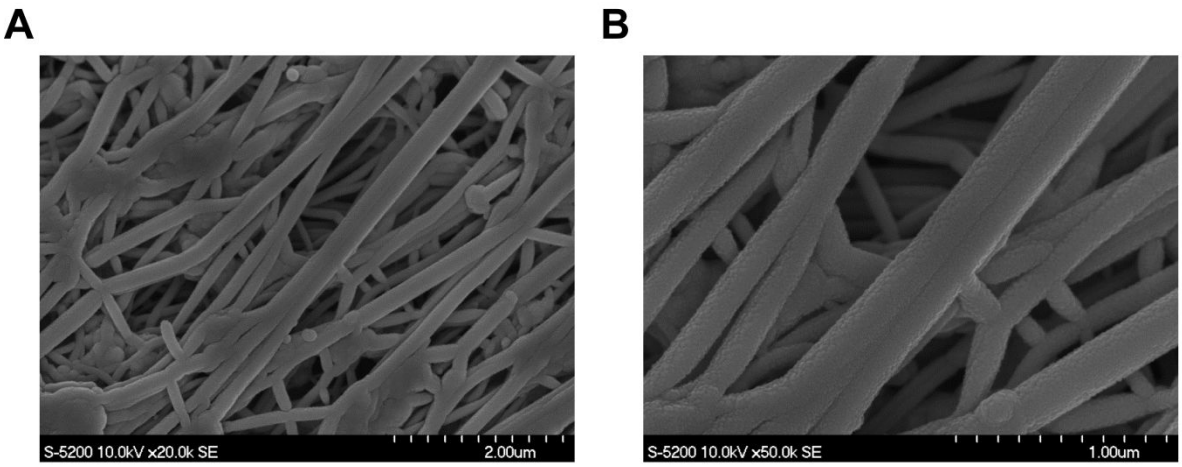

Figure S1. Morphology of Cu sputtered polytetrafluoroethylene (PTFE, 450 nm average pore size) gas diffusion layer (GDL) (reference Cu/PTFE electrode). (**A and B**) SEM images at different magnifications. The PTFE substrate maybe described best as a polymeric composite, in which arbitrarily and horizontally oriented PTFE fibers are bound to each other in a web-like matrix. The sputtered Cu surrounds the PTFE fibers conformably, forming an electronically conductive reaction region, whereas the macro-scale pores inherently formed between the fibers form pores, which enable pathways for the transport of the reactant and reaction products.

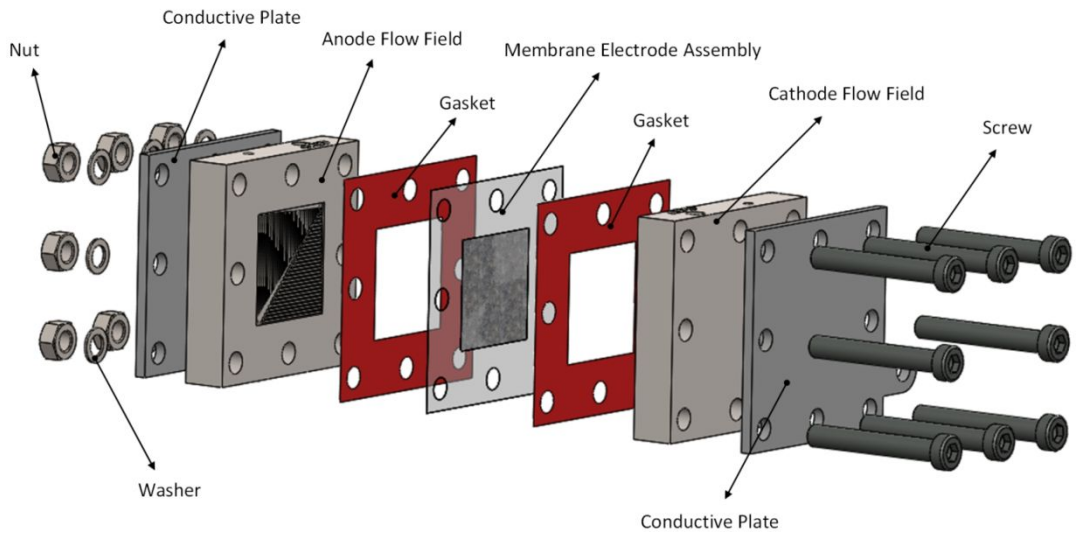

Figure S2. Schematic illustration of the CO_2RR membrane electrode assembly (MEA) electrolyzer. The main constituents of the CO_2 electrolyzer (Dioxide Materials) are membrane electrode assembly (MEA), anode and cathode flow fields (made of titanium and stainless steel, respectively), and anode and cathode conductive plates.

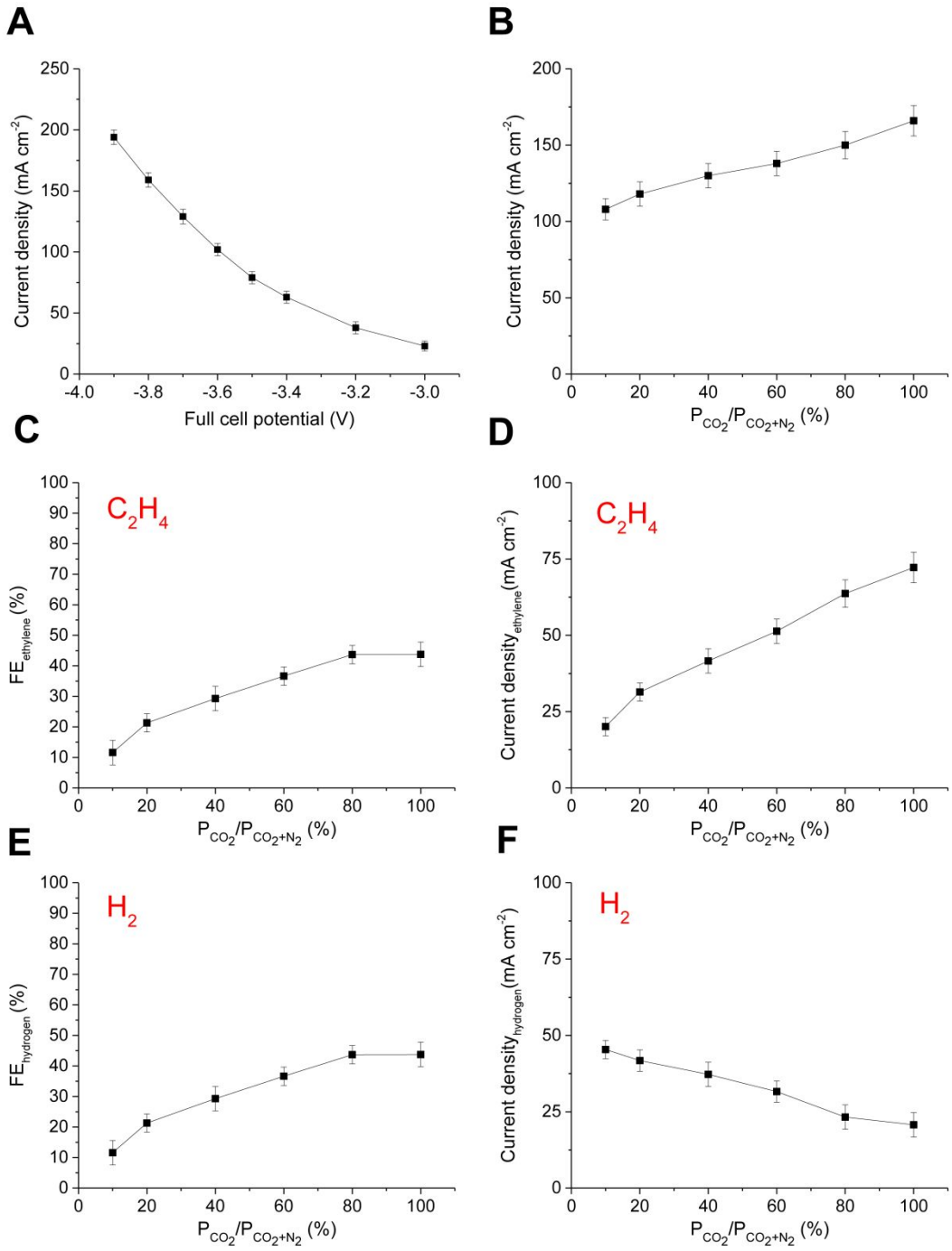

Figure S3. Effect of CO_2 availability on the electrochemical performance of the reference Cu/PTFE electrode. (A) Current densities obtained for the reference Cu/PTFE electrode. **(B)** Effect of CO_2 partial pressure on the current densities at a full-cell potential of -3.8 V. **(C)** Effect of CO_2 partial pressure on the C_2H_4 FEs at a full-cell potential of -3.8 V. **(D)** Effect of CO_2 partial

pressure on the ethylene partial current densities at a full-cell potential of -3.8 V. **(E)** Effect of CO_2 partial pressure on the H_2 FEs at a full-cell potential of -3.8 V. **(F)** Effect of CO_2 partial pressure on the hydrogen partial current densities at a full-cell potential of -3.8 V. Full-cell potentials are presented without iR compensation. Operating conditions of the MEA electrolyzer: 0.1 M $KHCO_3$ continuous anolyte was supplied to the anode side with the flow rate of 20 mL min^{-1}; fully humidified CO_2 was supplied to the cathode side with the flow rate of around 80 sccm; and cell temperature was kept constant at room temperature. Constrained CO_2 availability dominates the hydrogen evaluation reaction (HER) over the CO_2RR on the surface of the Cu/PTFE electrode, significantly limiting the current densities towards ethylene.

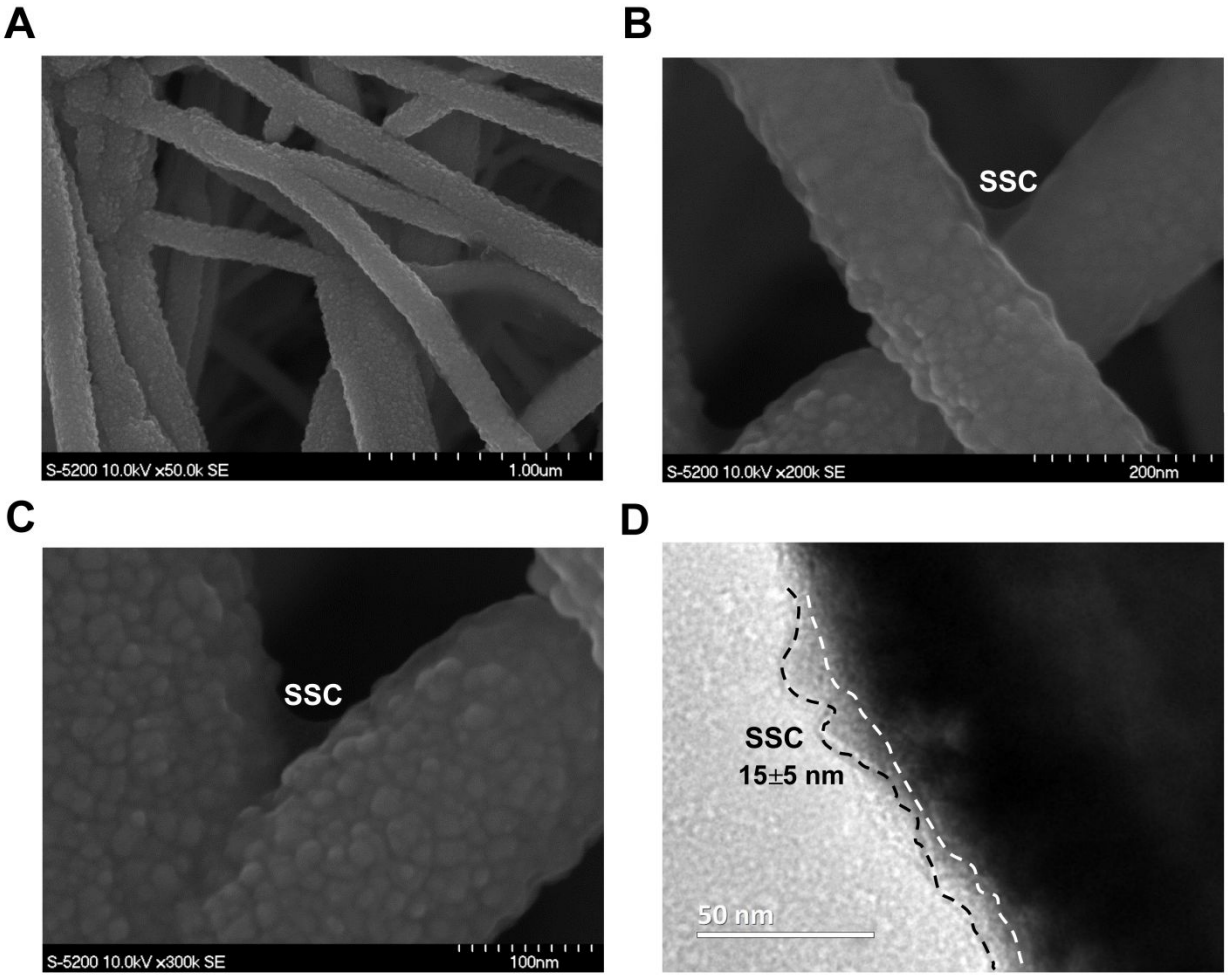

Figure S4. Morphology of SSC ionomer modified Cu/PTFE electrode. (A to C) SEM images at different magnifications. **(D)** TEM image at 50 nm. The SSC ionomer spray-deposited onto the Cu/PTFE electrode forms a 15±5 nm thick conformal layer on the surface of the Cu/PTFE fiber, which shrinks the mass transport layer to tens of nanometers and hence increases the CO_2 availability in the local chemical environment, enabling effective CO_2-to-ethylene conversion at high reaction rates (current densities). The mean thickness of 15±5 nm was calculated by averaging the thickness of the layers from five different SSC film coated fibers arbitrarily chosen from the different regions of the electrode. The Cu/PTFE fibers shown in the SEM images represent typical fibers of the Cu/PTFE electrode with a diameter of around 200 nm, and their thickness do not change significantly upon SSC ionomer modification.

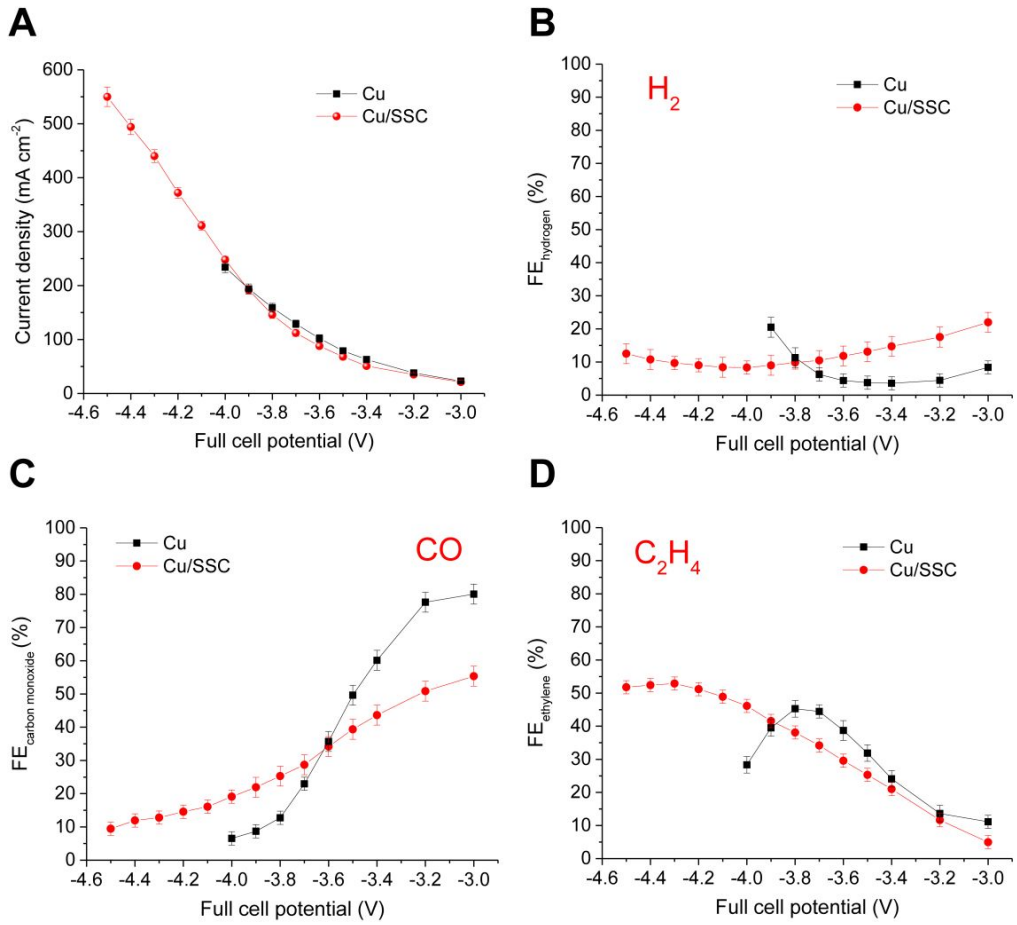

Figure S5. Effect of the SSC ionomer modification on the electrochemical performance of the reference Cu/PTFE electrode. (A) Current densities obtained for the reference Cu/PTFE electrode and SSC modified Cu/PTFE electrode. **(B)** Corresponding H_2. **(C)** Corresponding CO. **(D)** Corresponding C_2H_4 FE. Full-cell potentials are presented without iR compensation. Operating conditions of the MEA electrolyzer: 0.1 M $KHCO_3$ continuous anolyte was supplied to the anode side with the flow rate of 20 mL min^{-1}; fully humidified CO_2 was supplied to the cathode side with the flow rate of around 80 sccm; and cell temperature was kept constant at room temperature. The SSC ionomer modification suppresses the competing hydrogen evaluation reaction (HER); potentially increased CO_2 availability dominates CO_2RR over the HER. The SSC ionomer suppresses the overall CO generation at low full-cell potentials, but together with a

shift to the higher full-cell potential region, which facilitates its further reduction to ethylene at high full-cell potentials, enabling selective ethylene electrosynthesis up to current density of 550 mA/cm^{-2}, but along with the highly constrained energy efficiencies (EEs).

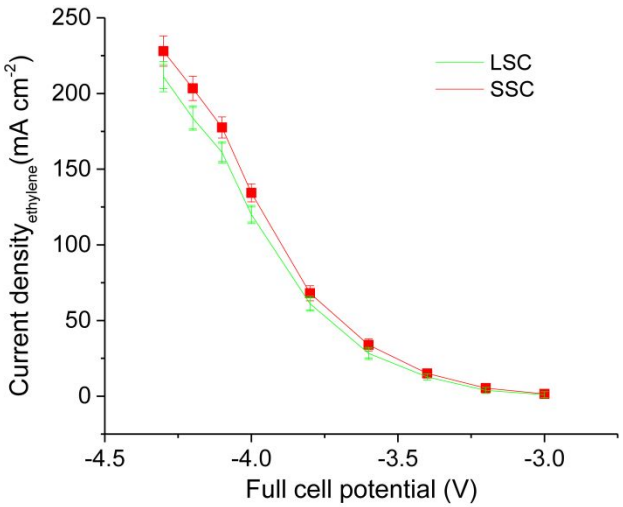

Figure S6. Effect of hydrophilic side chain length on the ethylene partial current densities. The cathode catalyst utilized was comprised of Cu NPs mixed with either LSC (Nafion®) or SSC (Aquivion® D79-25BS) supported on Cu/PTFE reference electrodes. The sputtered Cu thickness, Cu NPs loading, and Cu NPs:ionomer ratios were kept similar for both the catalysts. Full-cell potentials are presented without iR compensation. Operating conditions of the MEA electrolyzer: 0.1 M $KHCO_3$ continuous anolyte was supplied to the anode side with the flow rate of 20 mL min^{-1}; fully humidified CO_2 was supplied to the cathode side with the flow rate of around 80 sccm; and cell temperature was kept constant at room temperature.

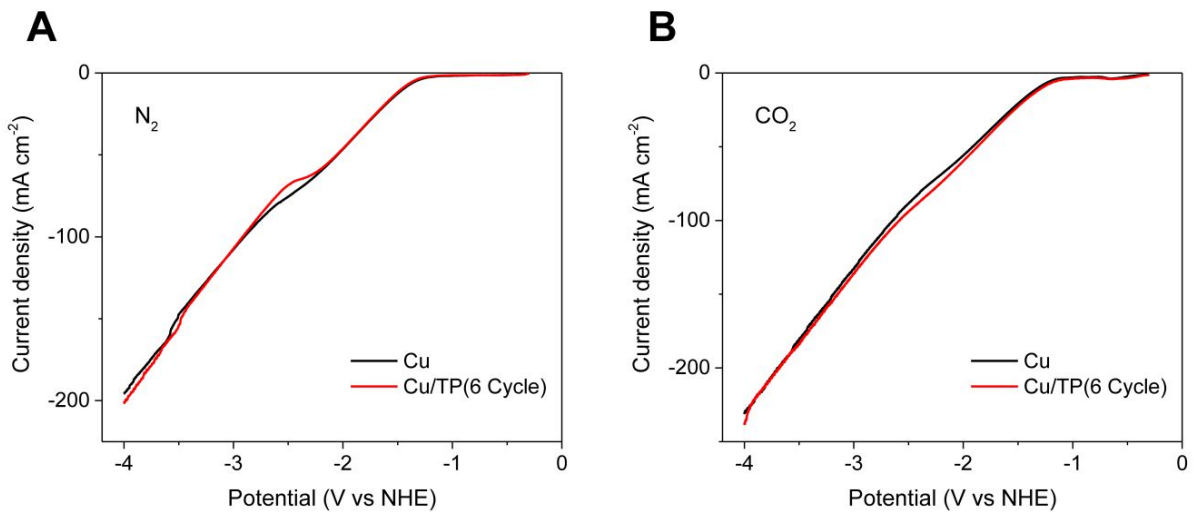

Figure S7. Linear sweep voltammetry curves of tetrahydro-phenanthrolinium film modified Cu/PTFE (Cu/TP) and reference Cu/PTFE (Cu) electrodes in a liquid-electrolyte flow cell system. (A) N_2 and **(B)** CO_2. Operating conditions: 1 M $KHCO_3$ continuous catholyte and anolyte were supplied to the cathode and anode side with the flow rate of 20 mL min^{-1}; gas (N_2 or CO_2) was supplied to the cathode side with the flow rate of around 80 sccm; and cell temperature was kept constant at room temperature. The linear sweep voltammetry curves were obtained by sweeping the voltage from -0.25 V to -4 V vs Ag/AgCl at a scan rate of 50 mV s^{-1}. Each curve is the representative of 15 scans from 3 independent measurements. For both the N_2 and CO_2 feeds, the reference Cu/PTFE and tetrahydro-phenanthrolinium modified Cu/PTFE yields similar current response. Specifically, when the CV measurement is performed under N_2 environment, only hydrogen evolution reaction (HER) occurs, and the current response under the same applied potentials for both the electrodes is the same, indicating that the tetrahydro-phenanthrolinium film modification does not block the catalytically active sites of the Cu catalyst.

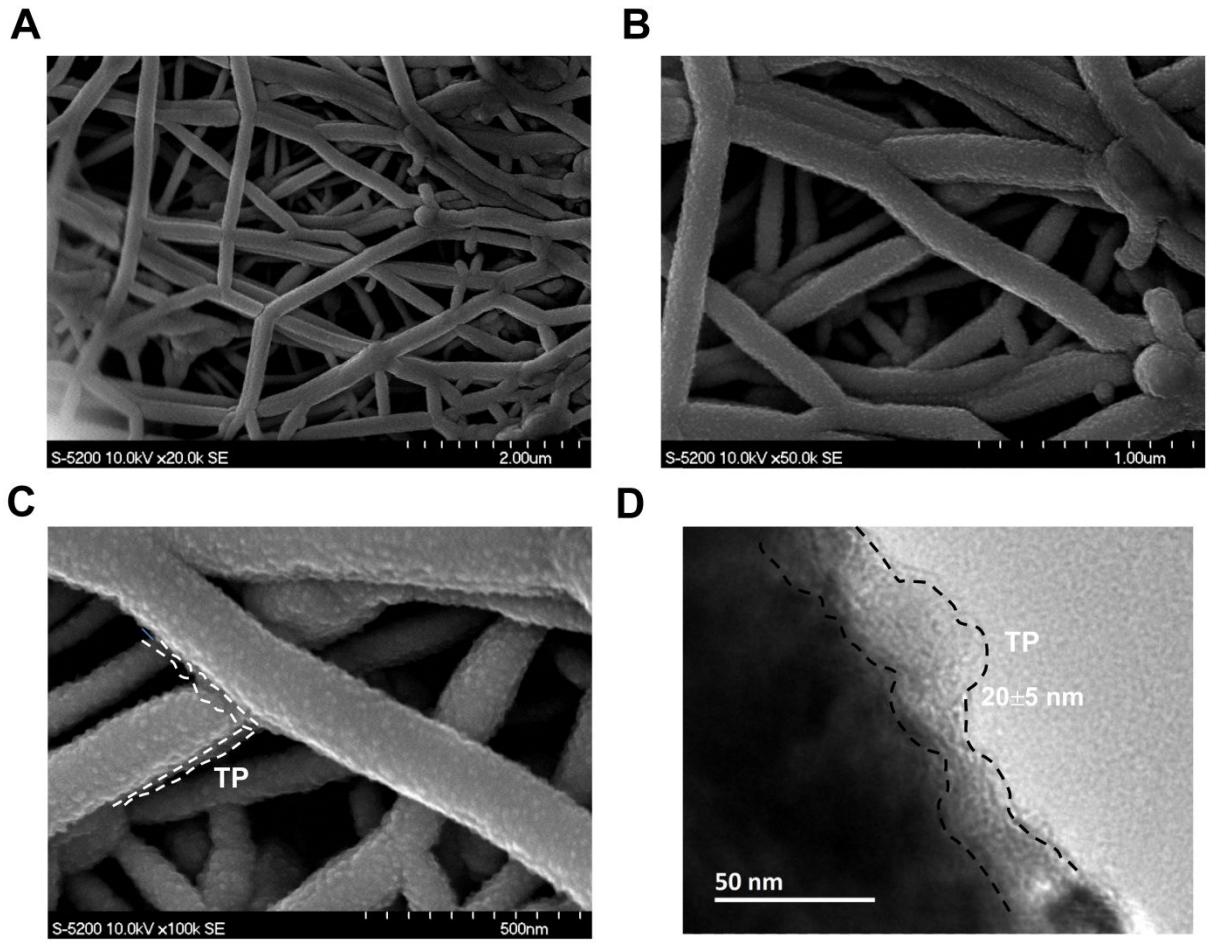

Figure S8. Morphology of tetrahydro-phenanthrolinium (TP) film modified Cu/PTFE electrode. (A to C) SEM images at different magnifications. **(D)** TEM image at 50 nm magnification. The TP film mean thickness of 20±5 nm was calculated by averaging the thickness of the layers from five different TP film coated fibers arbitrarily chosen from the different regions of the electrode. The Cu/PTFE fibers shown in the SEM images represent typical fibers of the Cu/PTFE electrode with a diameter of around 200 nm, and their thickness do not change significantly upon TP film modification.

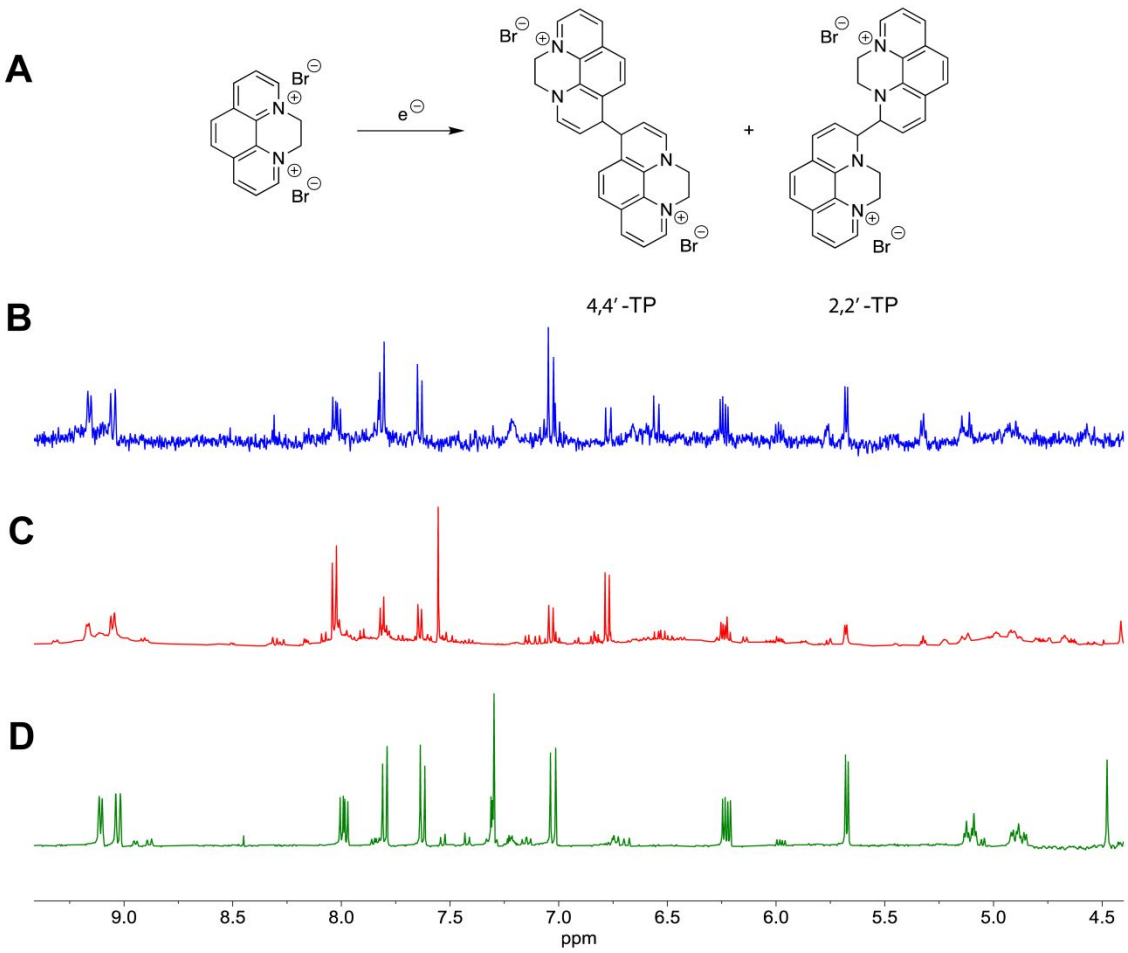

Figure S9. Electro-dimerization of N,N'-ethylene-phenanthrolinium dibromide molecular precursor onto the reference Cu/PTFE electrode. **(A)** Electrodimerization of the phenanthrolinium into the 4,4' and 2,2'-tetrahydro-phenanthrolinium dimeric structures.[1] **(B)** ^{1}H NMR spectrum of the obtained molecular film on the Cu/PTFE electrode immediately after electrodeposition. **(C)** ^{1}H NMR spectrum of the molecular film on the Cu/PTFE electrode after 2 weeks of electrodeposition. **(D)** For comparison, ^{1}H NMR spectrum of the obtained molecular film on a polycrystalline copper foil.[1]

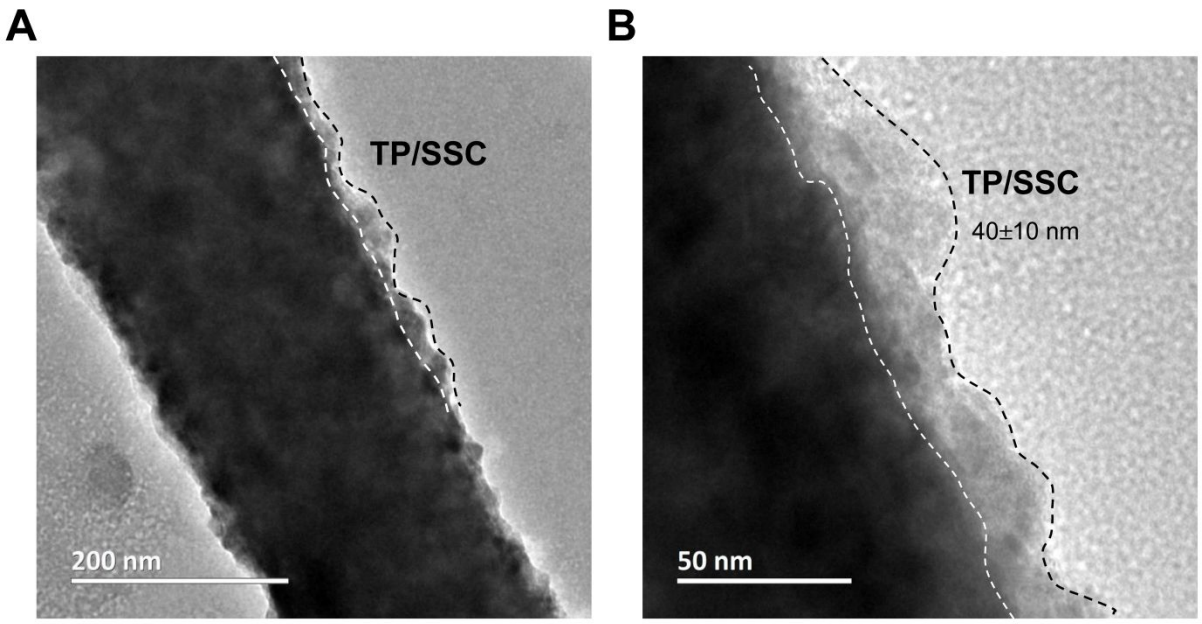

Figure S10. Morphology of tetrahydro-phenanthrolinium/SSC modification on reference Cu/PTFE electrode. (A and B) TEM images at different magnifications. The dashed black lines show the hierarchical ordering of tetrahydro-phenanthrolinium (TP) (inner layer enabled by electrodeposition) and SSC ionomer (outer layer enabled by spray deposition of SSC ionomer upon tetrahydro-phenanthrolinium electrodeposition) mix on Cu/PTFE fiber. The mean thickness of 40±10 nm was calculated by averaging the thickness of the layers from five different TP/SSC ionomer modified fibers arbitrarily chosen from the different regions of the electrode. The Cu/PTFE fiber shown in the images represents a typical fiber of the Cu/PTFE electrode with a diameter of around 200 nm, and its thickness does not change significantly upon TP/SSC ionomer modification.

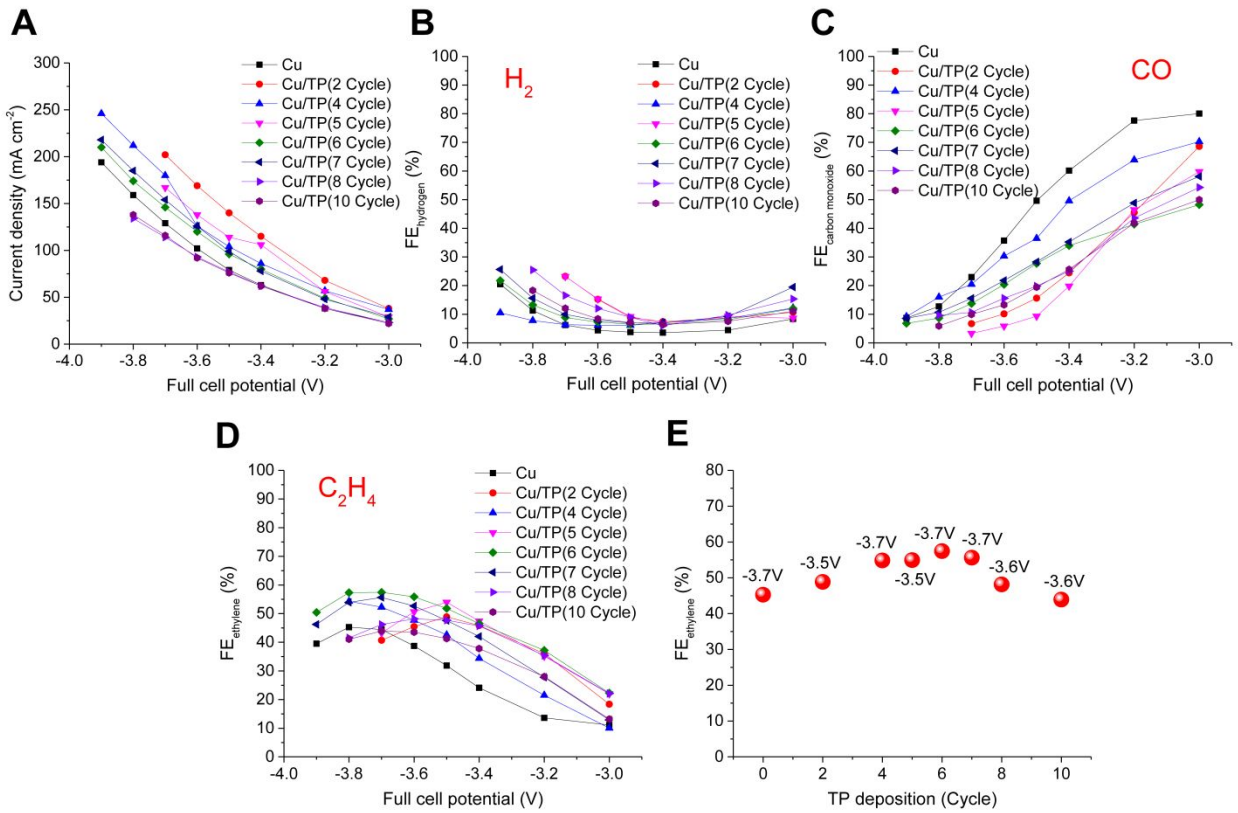

Figure S11. Optimization of the loading of tetrahydro-phenanthrolinium (TP) in the TP-modified Cu/PTFE electrode. (A) Current densities obtained for various cycles of electro-deposition. **(B)** Corresponding H_2 FE. **(C)** Corresponding CO FE. **(D)** Corresponding C_2H_4 FE. **(E)** Distribution of C_2H_4 FE and full-cell voltage for different electro-deposition cycles. The TP loading on Cu/PTFE is represented by the number of electro-deposition cycles. Full-cell potentials are presented without iR compensation. Operating conditions of the MEA electrolyzer: 0.1 M $KHCO_3$ continuous anolyte was supplied to the anode side with the flow rate of 20 mL min^{-1}; fully humidified CO_2 was supplied to the cathode side with the flow rate of around 80 sccm; and cell temperature was kept constant at room temperature. The TP electrodeposition on Cu/PTFE positively impacts the reaction rates (current densities), achieving a plateau at the intermediate electrodeposition cycles. With the electrodeposition of TP, depending on the number of cycles, the H_2 FEs show differences; however, the ideal number of electrodeposition cycles

does not cause a significant difference towards H_2 generation. Regardless of the number of cycles, the TP modification significantly suppresses CO, indicating that TP promotes CO adsorption on the Cu catalyst surface. Similarly, independent of the number of electrodeposition cycles, TP deposition promotes selectivity towards ethylene production – a finding suggesting that the improved CO adsorption promotes C-C coupling, and hence selective CO_2-to-ethylene conversion.

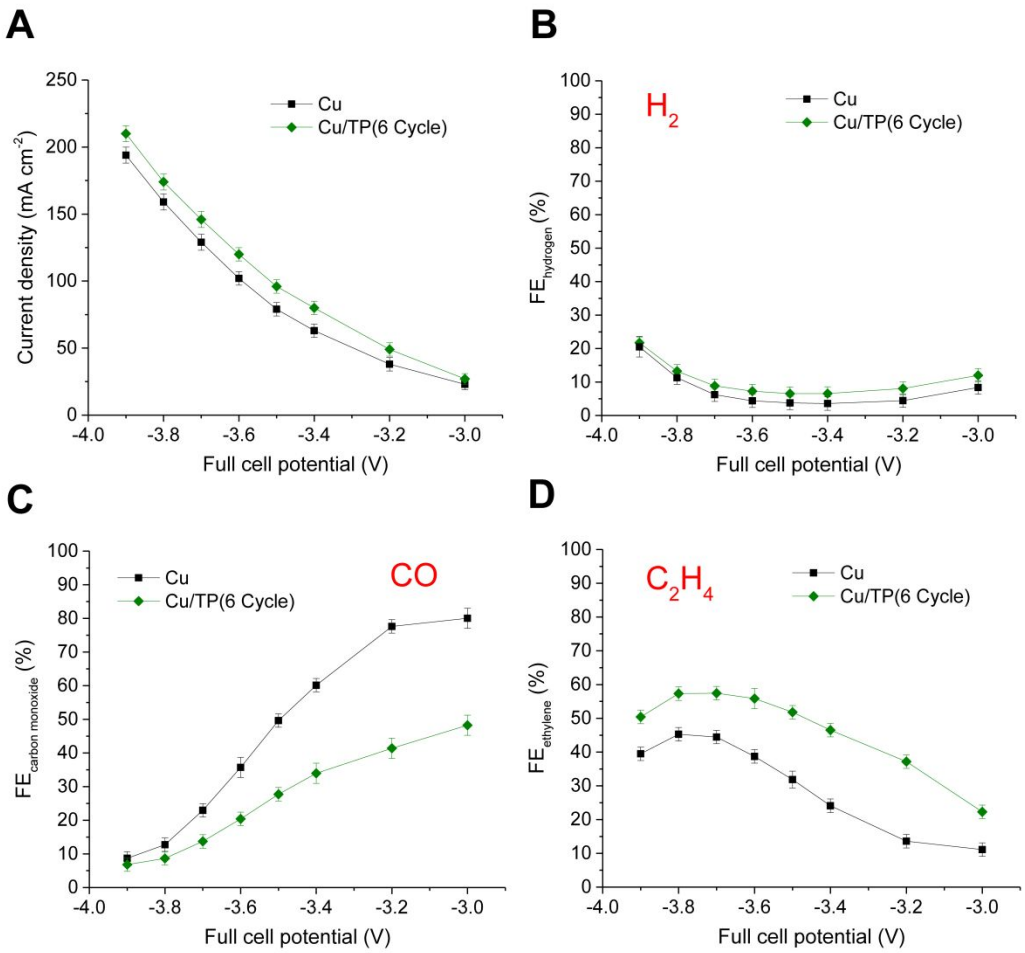

Figure S12. Effect of the tetrahydro-phenanthrolinium (TP) modification on the electrochemical performance of the reference Cu/PTFE electrode. (A) Current densities obtained for the reference Cu/PTFE electrode and tetrahydro-phenanthrolinium (TP) modified Cu/PTFE electrode. **(B)** Corresponding H_2 FE. **(C)** Corresponding CO FE. **(D)** Corresponding C_2H_4 FE. Full-cell potentials are presented without iR compensation. Operating conditions of the MEA electrolyzer: 0.1 M $KHCO_3$ continuous anolyte was supplied to the anode side with the flow rate of 20 mL min^{-1}; fully humidified CO_2 was supplied to the cathode side with the flow rate of around 80 sccm; and cell temperature was kept constant at room temperature. TP modification enables control over the adsorption energetics of *CO, promoting C-C coupling.

Thus, TP modification significantly suppresses the FE towards CO while promoting FE towards ethylene, compared to the unmodified Cu/PTFE.

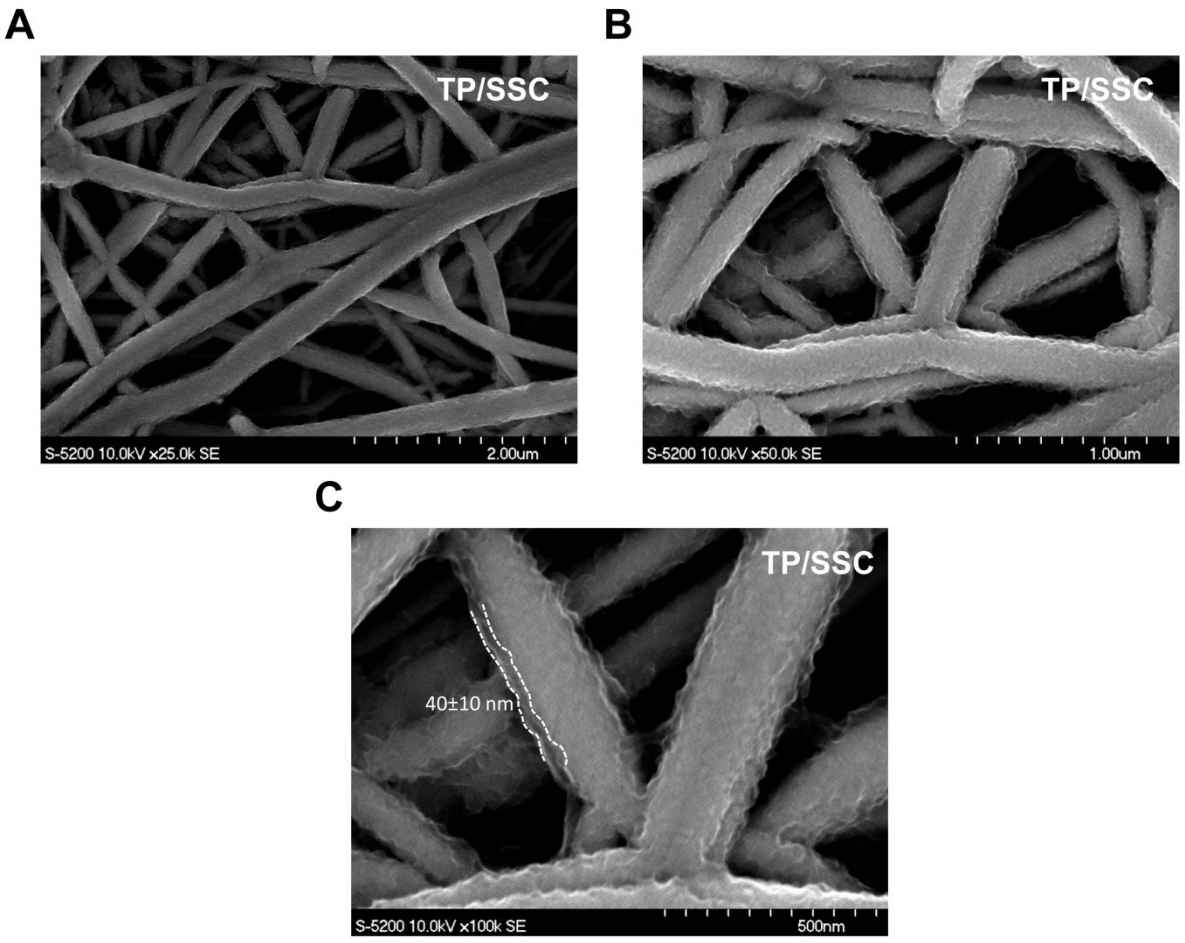

Figure S13. Morphology of the tetrahydro-phenanthrolinium/SSC ionomer modified Cu/PTFE electrode. (A to C) SEM images at different magnifications. The sequential tetrahydro-phenanthrolinium (TP) electrodeposition and SSC ionomer spray-deposition forms a 2D hierarchical reaction platform on the surface of Cu/PTFE. The resulting tetrahydro-phenanthrolinium/SSC ionomer 40±10 nm thick double-layer architecture forms conformal coverage throughout the surface of Cu/PTFE. The region between the white dashed lines represents the thickness of the hierarchical TP/SSC layers on the Cu/PTFE fiber. The mean thickness of 40 nm was calculated by averaging the thickness of five different TP/SSC ionomer modified fibers arbitrarily chosen from the different regions of the electrode.

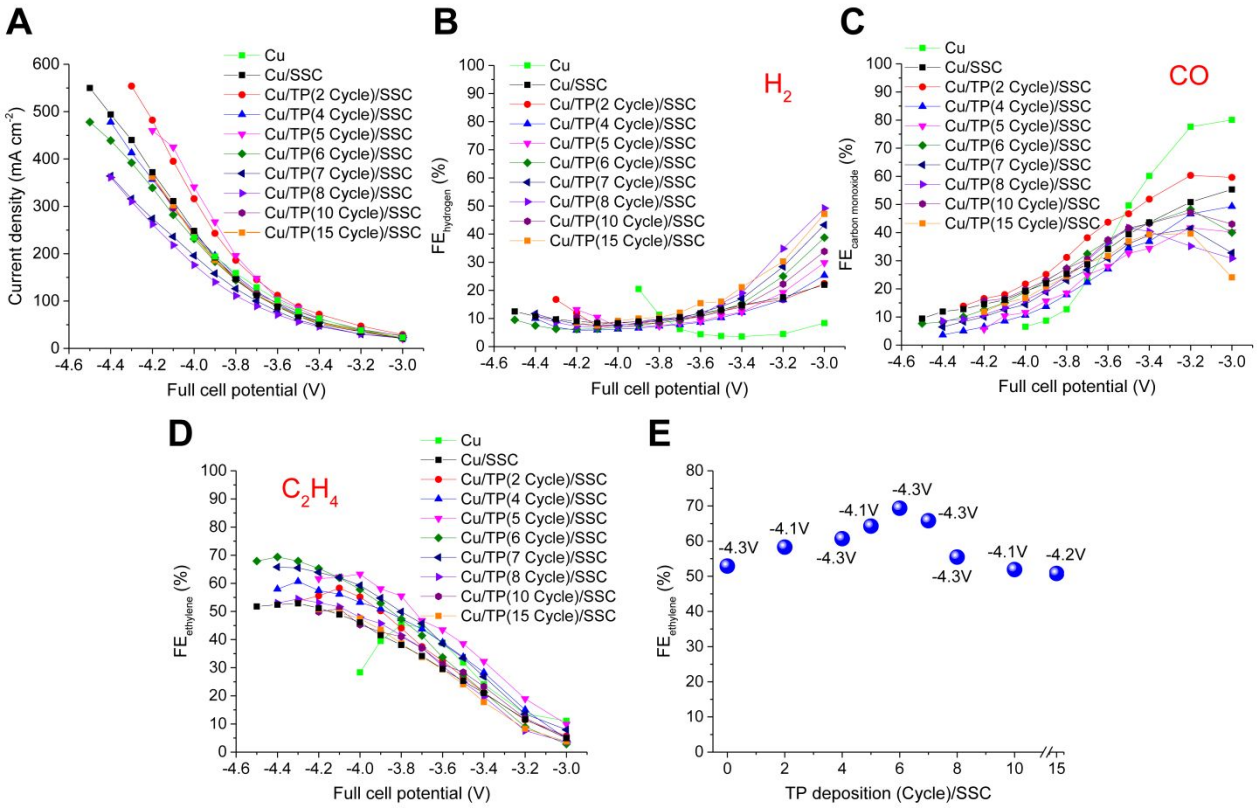

Figure S14. Optimization of the loading of the tetrahydro-phenanthrolinium (TP) in the Cu/ tetrahydro-phenanthrolinium/ionomer modification of the catalyst. (A) Current densities obtained for various cycles of electro-deposition. **(B)** Corresponding H_2 FE. **(C)** Corresponding CO FE. **(D)** Corresponding C_2H_4 FE. **(E)** Distribution of C_2H_4 FE and full-cell potential for various cycles of tetrahydro-phenanthrolinium electro-deposition. The tetrahydro-phenanthrolinium loading on the reference Cu/PTFE electrode is represented by the number of electro-deposition cycles. Full-cell potentials are presented without iR compensation. Operating conditions of the MEA electrolyzer: 0.1 M $KHCO_3$ continuous anolyte was supplied to the anode side with the flow rate of 20 mL min^{-1}; fully humidified CO_2 was supplied to the cathode side with the flow rate of around 80 sccm; and cell temperature was kept constant at around room temperature.

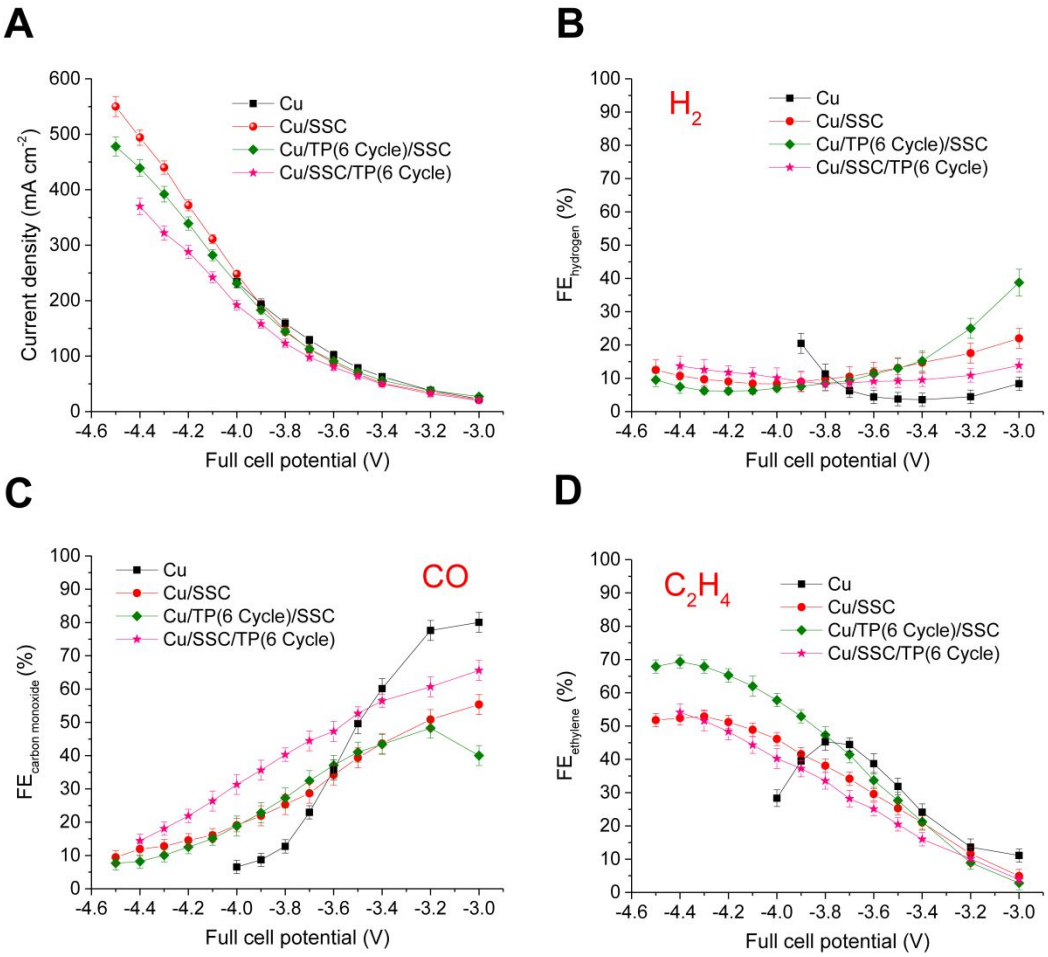

Figure S15. Effect of the deposition ordering of tetrahydro-phenanthrolinium (TP) and SSC ionomer in the 2D CTPI catalyst. (A) Current densities of the reference Cu/PTFE electrode, SSC ionomer modified Cu/PTFE electrode (Cu/SSC), tetrahydro-phenanthrolinium:SSC ionomer modified Cu/PTFE electrode (Cu/TP(6 Cycle)/SSC), and SSC ionomer:tetrahydro-phenanthrolinium modified Cu/PTFE electrode (Cu/SSC/TP(6 Cycle)). **(B)** Corresponding H_2 FE. **(C)** Corresponding CO FE. **(D)** Corresponding C_2H_4 FE. Full-cell potentials are presented without iR compensation. Operating conditions of the MEA electrolyzer: 0.1 M $KHCO_3$ continuous anolyte was supplied to the anode side with the flow rate of 20 mL min^{-1}; fully humidified CO_2 was supplied to the cathode side with the flow rate of around 80 sccm; and cell temperature was kept constant at room temperature. The establishment of correct tetrahydro-

phenanthrolinium/SSC ionomer hierarchy on Cu/PTFE is a key for selective and high-rate CO_2-to-ethylene conversion. When the tetrahydro-phenanthrolinium has no conformal interaction with the Cu catalyst surface, it can neither successfully suppress the CO generation nor yield highly selective ethylene conversion – a finding showing that the tetrahydro-phenanthrolinium should conformably cover the Cu surface to enable efficient control over the adsorption energetics of *CO, and hence ethylene production. Similarly, when the SSC ionomer is spray-deposited onto the Cu/PTFE prior to tetrahydro-phenanthrolinium electro-deposition, its function in CO_2 transport (hence improving reaction rates and suppressing the HER) is constrained to a large extent. Thus, to successfully combine high-reaction rates with selectivity, the tetrahydro-phenanthrolinium should be electrodeposited on Cu/PTFE surface prior to spray-deposition of the SSC ionomer.

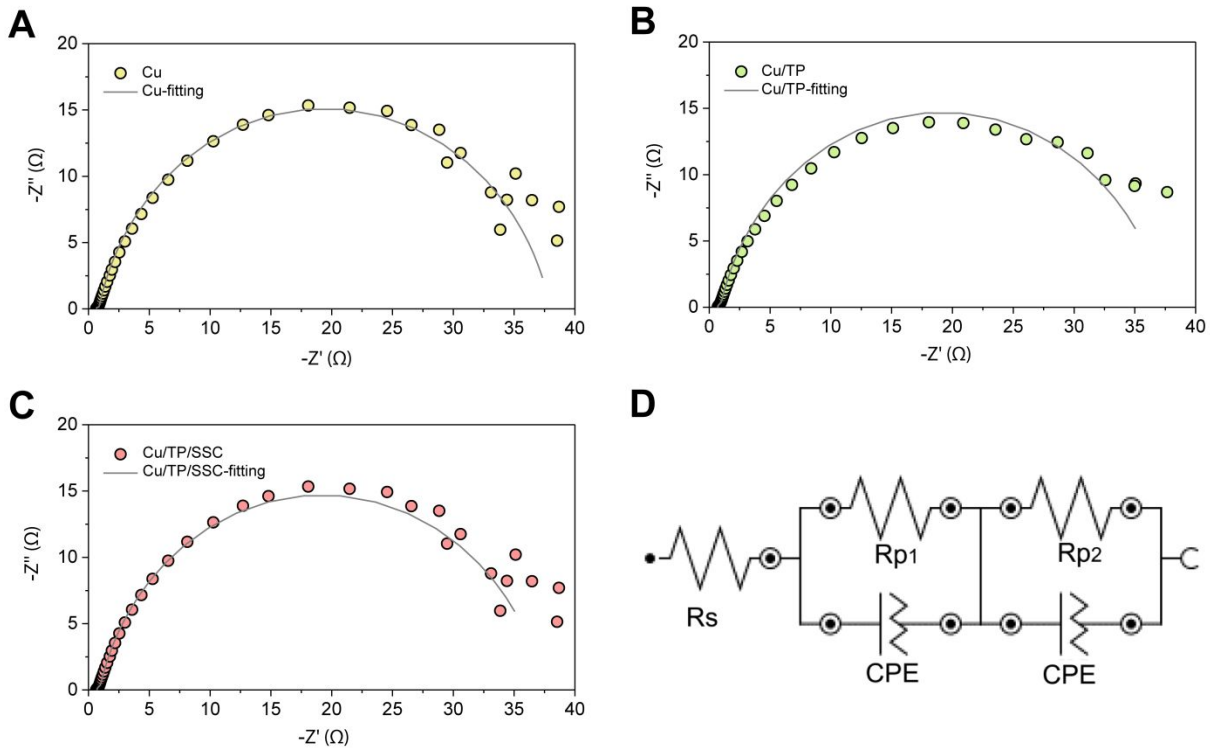

Figure S16. Electrochemical impedance spectroscopy (EIS) measurements of the MEA electrolyzers equipped with different cathode electrodes. (A) Reference Cu/PTFE electrode (Cu). **(B)** Tetrahydro-phenanthrolinium modified Cu/PTFE (Cu/TP). **(C)** Tetrahydro-phenanthrolinium:SSC ionomer modified Cu/PTFE (Cu/TP(6 Cycle)/SSC)**. (D)** The equivalent circuit for the fitting data. R_s represents the solution resistance, and $R_{p(s)}$ represent the charge transfer resistance at different interfaces. The EIS measurements used the same anolyte, CO_2 flow rate, and temperature (room temperature) for operating CO_2RR. The cathodic electrodes were first reduced in an MEA electrolyzer at -1.6 V for 15 min. The EIS measurements were then performed under the same condition. The anolyte was kept stationary during the measurements. The EIS measurements revealed that the introduction of tetrahydro-phenanthrolinium and SSC ionomer layers has a negligible impact on the electrochemical impedance of the CO_2RR using different electrodes (see also Table S1).

Table S1. Summary of the solution and charge resistances for the MEA electrolyzers equipped with different cathode electrodes.

Cathode	Rs (Ω)	Rp_1 (Ω)	Rp_2 (Ω)
Cu	0.638	0.217	37.1
Cu/TP(6 Cycle)	0.697	0.228	36.5
Cu/TP(6 Cycle)/SSC	0.639	0.283	36.1

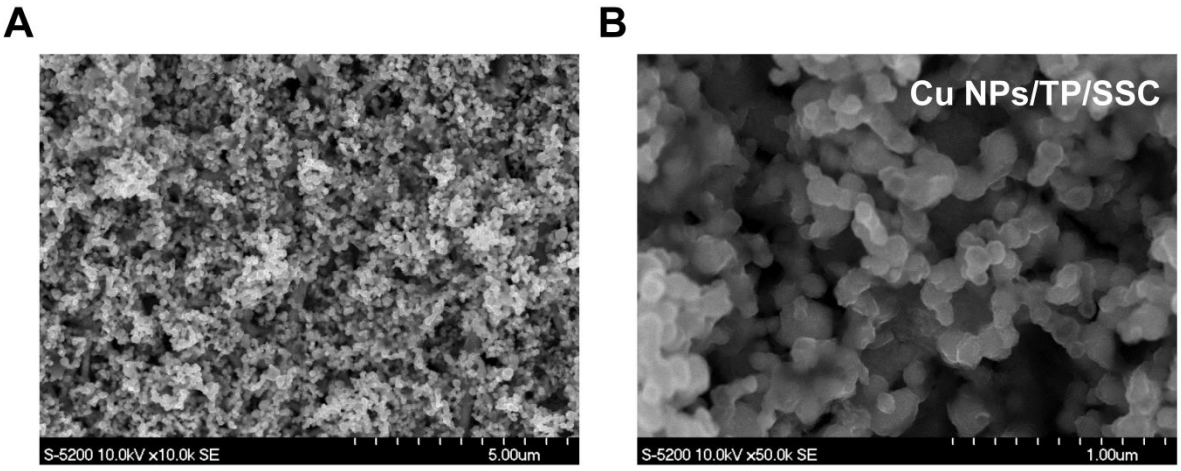

Figure S17. Morphology of the 3D CTPI catalyst comprised of arbitrarily dispersed Cu NPs/tetrahydro-phenanthrolinium/SSC ionomer mix on the reference Cu/PTFE electrode before the CO_2RR. (A and B) SEM images at different magnifications.

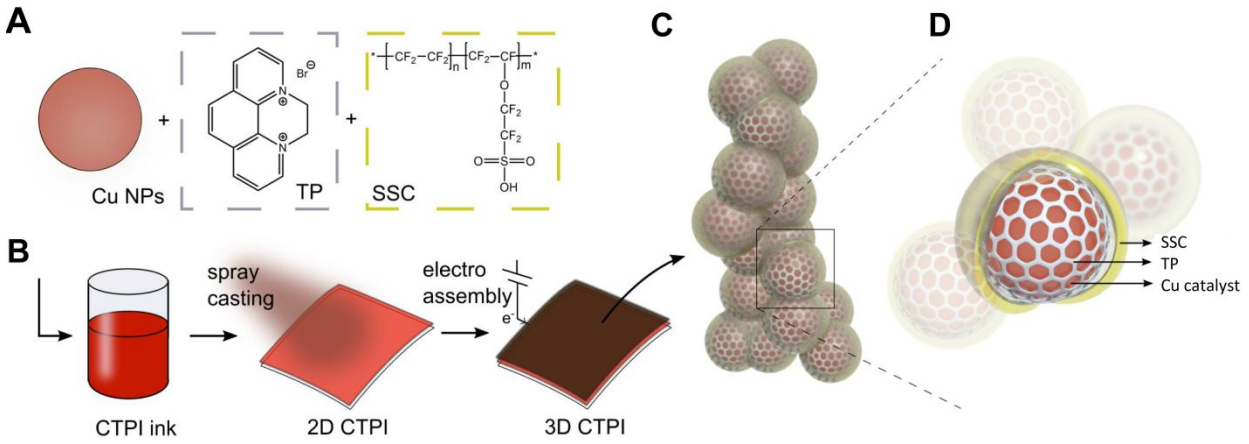

Figure S18. Schematic illustration of 3D CTPI catalyst. (A) Mechanical and ultrasonic mixing the ink comprised of Cu NPs, N, N'-ethylene-phenanthrolinium dibromide precursor, and SSC ionomer. **(B)** Spray-casting of the catalyst ink onto the 2D CTPI to establish the 3D CTPI under the negative bias formed on the cathode during CO_2RR. **(C)** Schematic illustration of the Cu NPs surrounded by the tetrahydro-phenanthrolinium:SSC ionomer heterojunction. **(D)** Cu NPs surrounded sequentially by the tetrahydro-phenanthrolinium and SSC ionomer layers. We utilized the electrodepositability of N,N'-ethylene-phenanthrolinium dibromide molecular precursor to establish the correct hierarchy of tetrahydro-phenanthrolinium/SSC ionomer together with Cu NPs on Cu/PTFE. We first prepared the slurries by mixing N,N'-ethylene-phenanthrolinium dibromide molecular precursor, Cu NPs, and SSC ionomer in polar solvents, and upon completion of 1 h of continuous ultrasonic mixing, we then spray-deposited the homogeneously dispersed catalyst slurries onto Cu/PTFE substrates. After complete drying of the resulting electrodes, we then assembled them into the MEA electrolyzer and initiated the CO_2RR, under which the negative bias formed on the cathode electrode electro-dimerized the molecular precursor, establishing highly porous reaction platform comprised of Cu NPs/tetrahydro-phenanthrolinium/SSC ionomer mix.

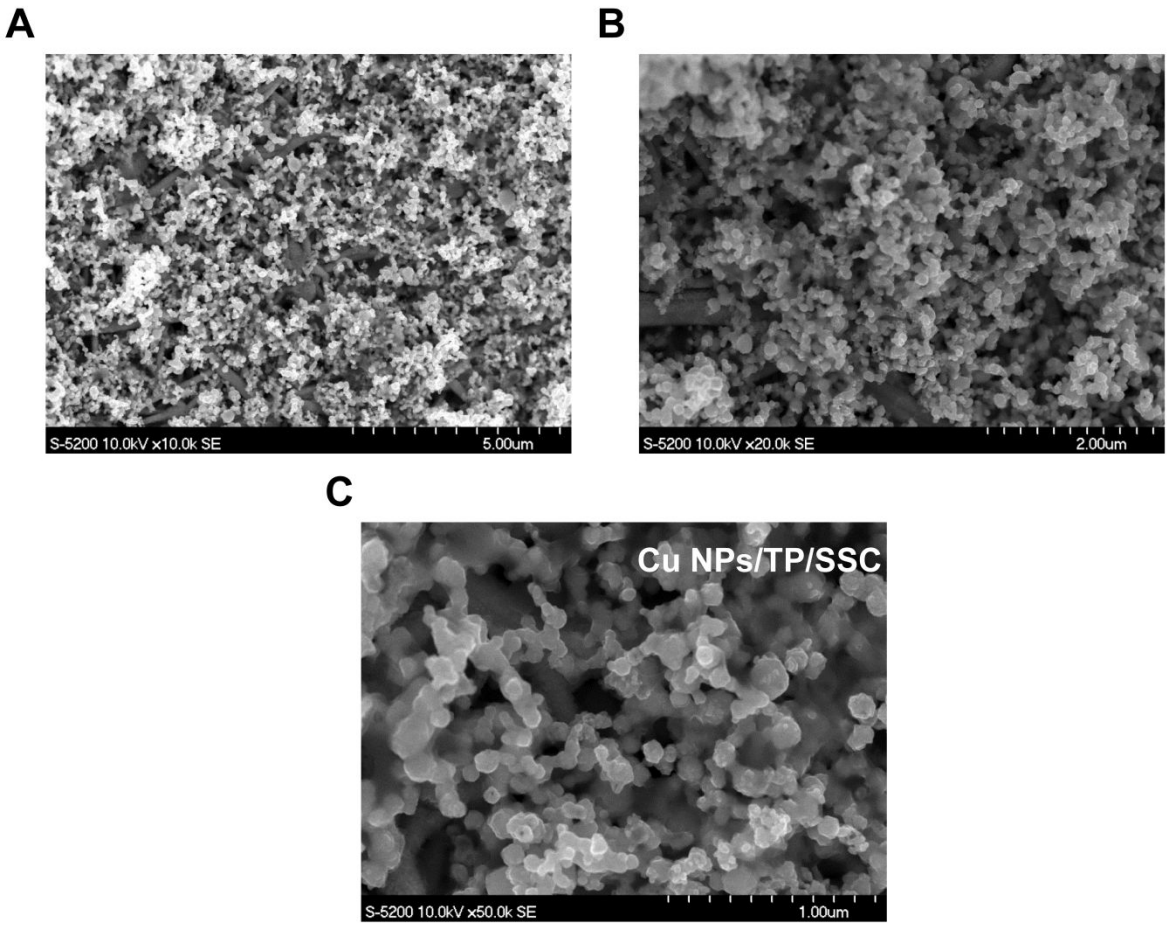

Figure S19. Morphology of the post-mortem 3D CTPI catalyst comprised of hierarchical Cu NPs/tetrahydro-phenanthrolinium/SSC ionomer ordering established upon completion of electrolysis in MEA electrolyzer. (A to C) SEM images at different magnifications.

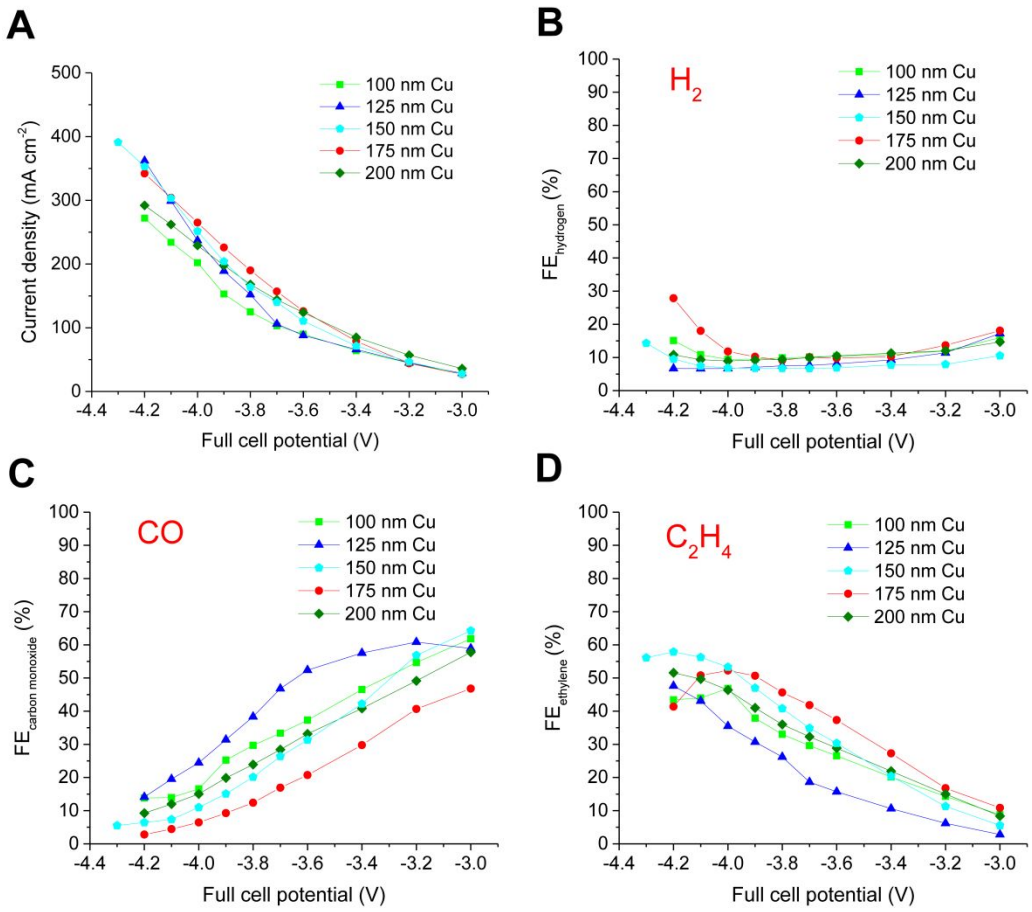

Figure S20. Optimization of the sputtered Cu thickness in 3D catalyst configuration. (A) Current densities obtained for various sputtered Cu thicknesses. **(B)** Corresponding H_2 FE. **(C)** Corresponding CO FE. **(D)** Corresponding C_2H_4 FE. The Cu NPs loading and Cu-to-ionomer weight ratio (wt%) were kept constant at 1.25 mg cm^{-2} and 22%, respectively. Full-cell potentials are presented without iR compensation. Operating conditions of the MEA electrolyzer: 0.1 M $KHCO_3$ continuous anolyte was supplied to the anode side with the flow rate of 20 mL min^{-1}; fully humidified CO_2 was supplied to the cathode side with the flow rate of around 80 sccm; and experiments were carried out at room temperature.

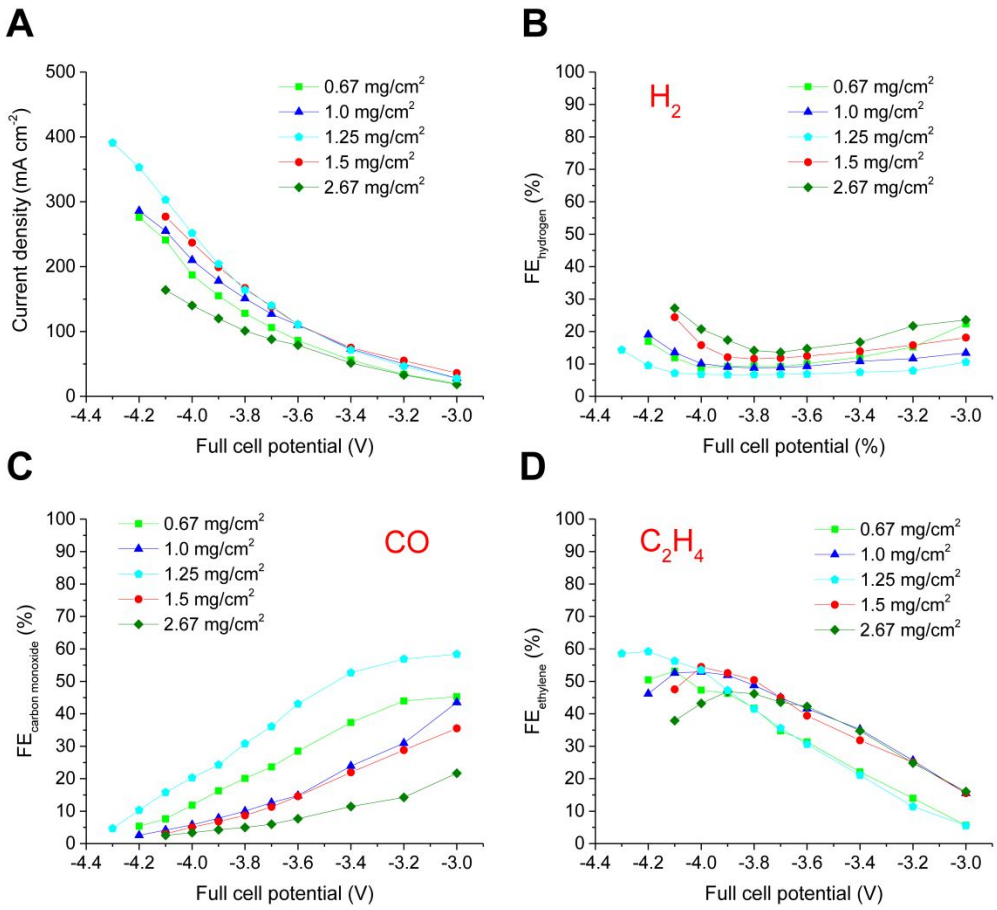

Figure S21. Optimization of the Cu NPs loading in the 3D catalyst configuration. (A) Current densities obtained for various Cu NPs loadings. **(B)** Corresponding H_2 FE. **(C)** Corresponding CO FE. **(D)** Corresponding C_2H_4 FE. The sputtered Cu thickness and Cu-to-ionomer weight ratio (wt%) were kept constant at 150 nm and 22%, respectively. Full-cell potentials are presented without iR compensation. Operating conditions of the MEA electrolyzer: 0.1 M $KHCO_3$ continuous anolyte was supplied to the anode side with the flow rate of 20 mL min^{-1}; fully humidified CO_2 was supplied to the cathode side with the flow rate of around 80 sccm; and cell temperature was kept constant at room temperature. The Cu nanoparticles (Cu NPs) loading on the Cu/PTFE substrate significantly impacts the reaction rate and selectivity of CO_2-to-ethylene conversion in the MEA electrolyzer. An increase in the nominal Cu NPs loading causes an improvement in the current density, achieving a plateau at the nominal loading of 1.25

mg/cm^2, and any further increase in the loading causes a significant drop in the current density, attributable to the restricted CO_2 transport because of the less porous (more compact) electrode microstructure formed – in good agreement with the elevated H_2 generation observed for the NPs loadings higher than 1.25 mg/cm^2. For this nominal Cu NPs loading, the 3D reaction platform also becomes more selective to ethylene, likely due to the suppressed H_2 generation.

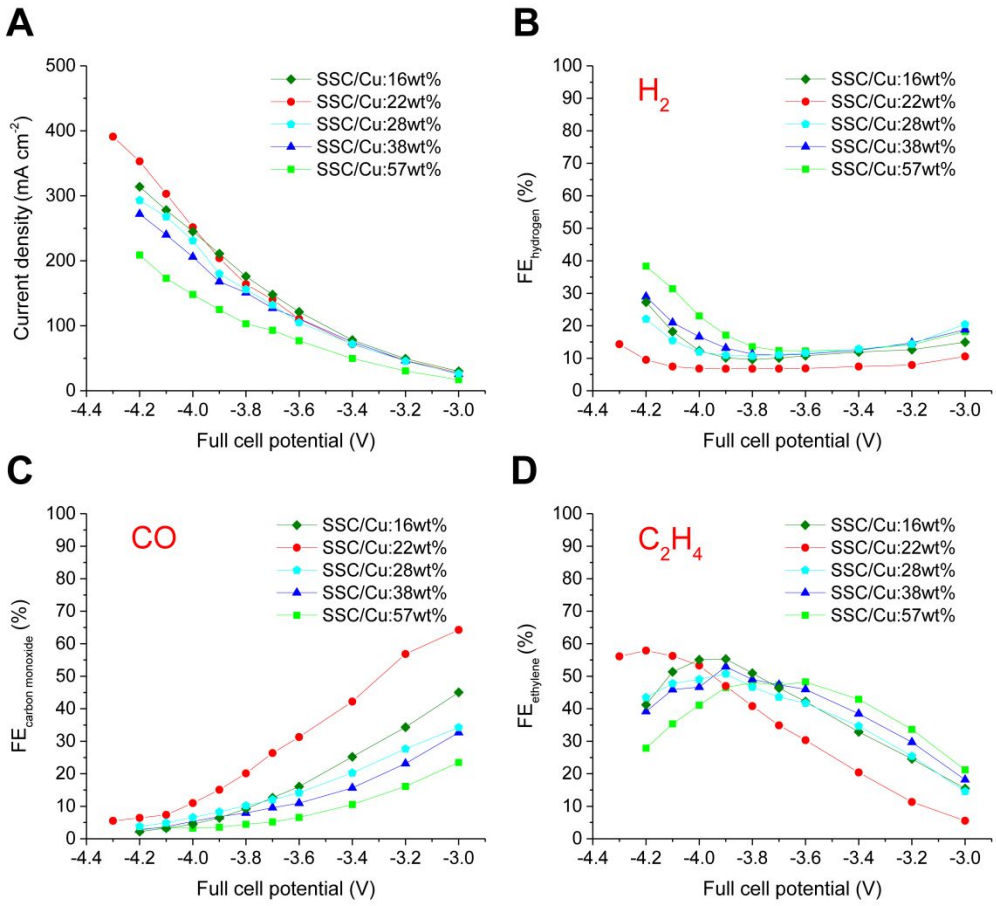

Figure S22. Optimization of the Cu-to-ionomer weight ratio (wt%) in the 3D catalyst configuration. (A) Current densities obtained for various Cu-to-ionomer weight ratios (wt%). **(B)** Corresponding H_2 FE. **(C)** Corresponding CO FE. **(D)** Corresponding C_2H_4 FE. The sputtered Cu thickness and Cu NPs loading were kept constant at 150 nm and 1.25 mg cm^{-2}, respectively. Full-cell potentials are presented without iR compensation. Operating conditions of the MEA electrolyzer: 0.1 M $KHCO_3$ continuous anolyte was supplied to the anode side with the flow rate of 20 mL min^{-1}; fully humidified CO_2 was supplied to the cathode side with the flow rate of around 80 sccm; and cell temperature was kept constant at room temperature. The blend ratio of Cu NPs/SSC ionomer in 3D configuration significantly impacts the reaction rate and selectivity of CO_2-to-ethylene conversion in the MEA electrolyzer. The ideal SSC ionomer to Cu NPs weight ratio of 22% suppresses hydrogen evaluation reaction (HER) and promotes ethylene

generation. The 3D configuration with the ideal Cu NPs/SSC ionomer blend ratio provides ethylene selectivity of 57% at around 355 mA/cm^2, suggesting that the blend ratio is important for the establishment of desirable local chemical environment and improved CO_2 transport.

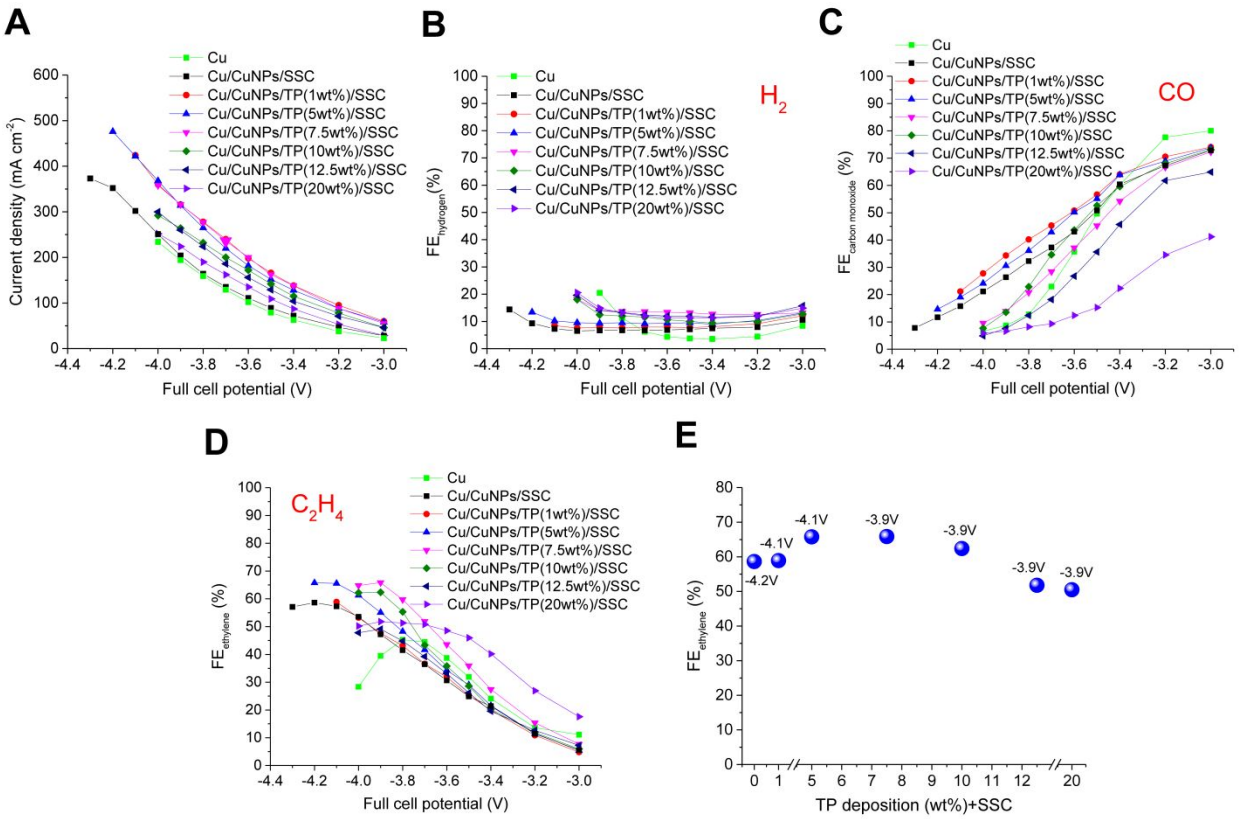

Figure S23. Optimization of the tetrahydro-phenanthrolinium (TP) loading in the 3D CTPI catalyst. (A) Current densities obtained for various cycles of electro-deposition. **(B)** Corresponding H_2 FE. **(C)** Corresponding CO FE. **(D)** Corresponding C_2H_4 FE. **(E)** Distribution of C_2H_4 FE and full-cell potential for the weight percentage of tetrahydro-phenanthrolinium to the Cu NPs loading. The tetrahydro-phenanthrolinium loading in the reaction platform is represented by the relative weight ratio (wt%) of the tetrahydro-phenanthrolinium to that of Cu NPs. For selective, high-rate and efficient CO_2-to-ethylene conversion, we determined the ideal wt% between the tetrahydro-phenanthrolinium/Cu NPs to be 7.5%. Full-cell potentials are presented without iR compensation. Operating conditions of the MEA electrolyzer: 0.1 M $KHCO_3$ continuous anolyte was supplied to the anode side with the flow rate of 20 mL/min; fully humidified CO_2 was supplied to the cathode side with the flow rate of around 80 sccm; and cell temperature was kept constant at around room temperature.

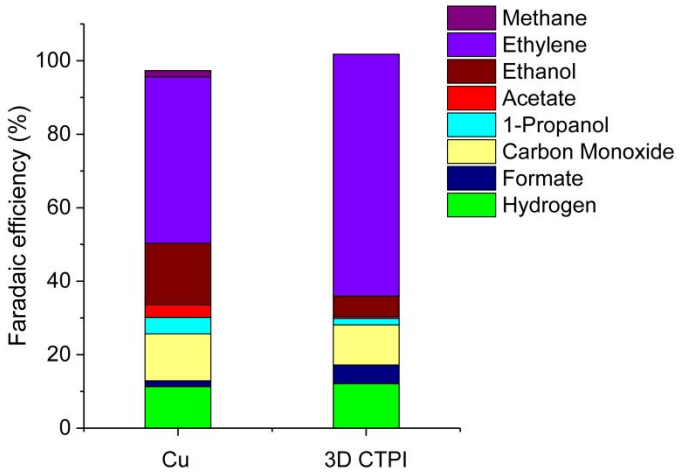

Figure S24. CO_2RR product distribution of the reference Cu/PTFE and 3D CTPI catalyst. The product spectra of both the Cu/PTFE and 3D CTPI catalyst were obtained by applying constant current densities that enable the highest ethylene FE, which were around 150 mA cm^{-2} and 300 mA cm^{-2}, respectively. Operating conditions of the MEA electrolyzer: 0.1 M $KHCO_3$ continuous anolyte was supplied to the anode side with the flow rate of 20 mL min^{-1}; fully humidified CO_2 was supplied to the cathode side with the flow rate of around 80 sccm; and cell temperature was kept constant at around room temperature.

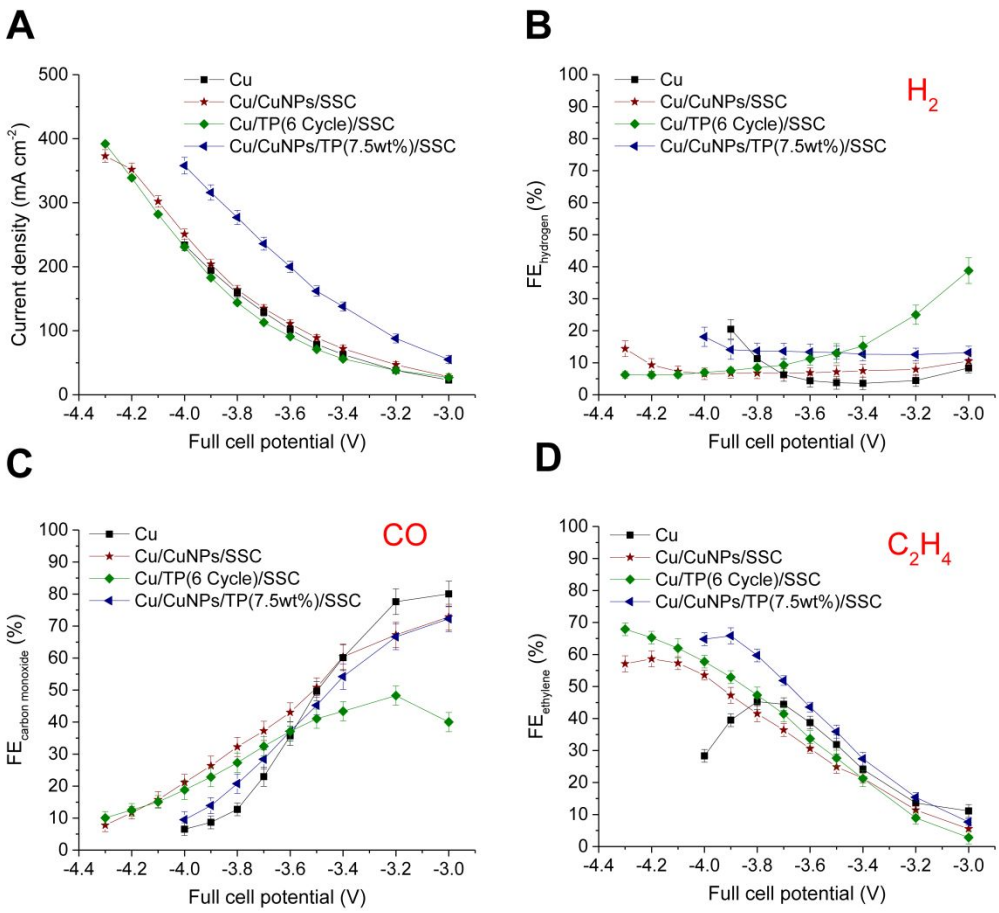

Figure S25. CO_2RR performance comparison between 2D Cu/PTFE (Cu), tetrahydro-phenanthrolinium/SSC on Cu/PTFE (Cu/TP(6 Cycle)/SSC), 3D Cu NPs/SSC ionomer on Cu/PTFE (Cu/Cu NPs/SSC), and Cu NPs/tetrahydro-phenanthrolinium/SSC ionomer on Cu/PTFE (Cu/Cu NPs/TP(7.5wt%)/SSC). (A) Comparison of current densities. **(B)** Corresponding H_2 FE. **(C)** Corresponding CO FE. **(D)** Corresponding C_2H_4 FE. 3D CTPI hierarchical reaction platform yields comparable selectivity compared to the 2D hierarchical reaction platform, along with the advantageous of much higher reaction rates at similar full-cell potentials. Full-cell potentials are presented without iR compensation. Operating conditions of the MEA electrolyzer: 0.1 M $KHCO_3$ continuous anolyte was supplied to the anode side with the flow rate of 20 mL min^{-1}; fully humidified CO_2 was supplied to the cathode side with the flow rate of around 80 sccm; and cell temperature was kept constant at around room temperature.

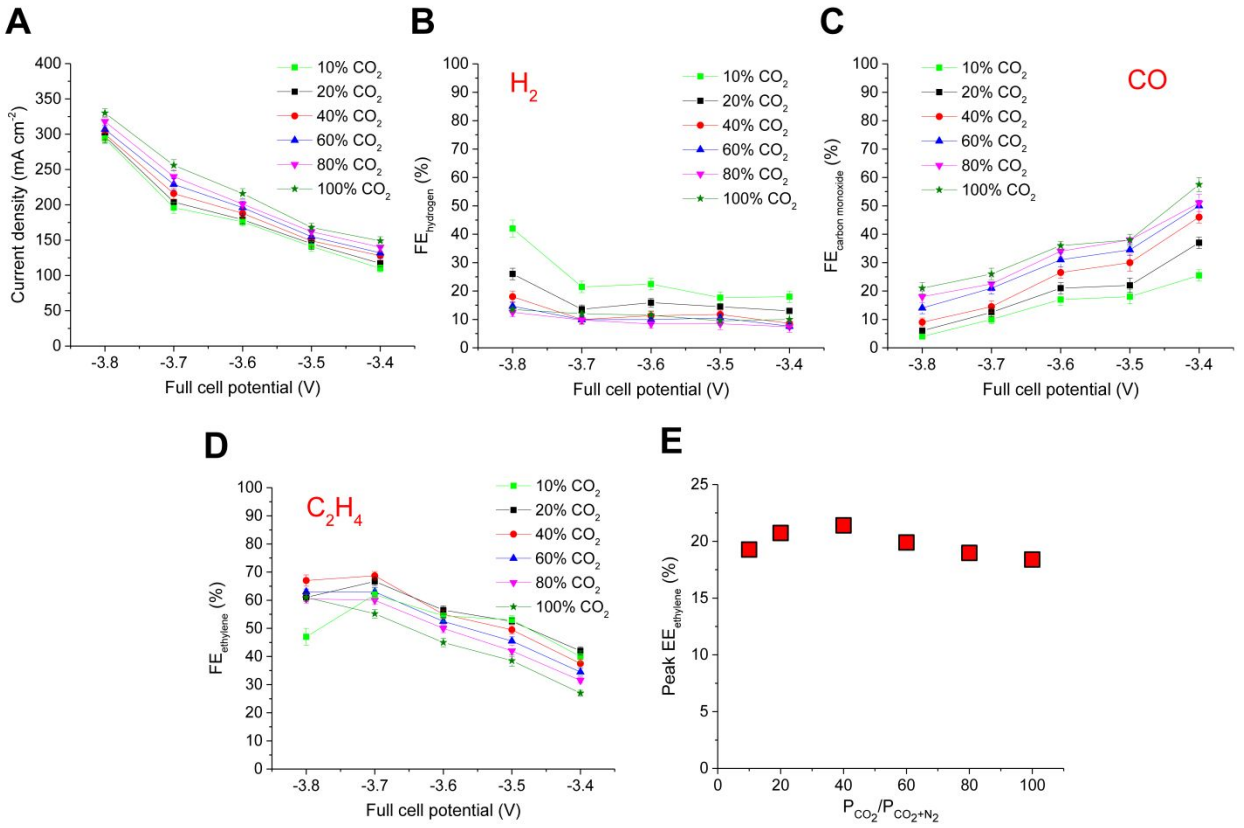

Figure S26. CO_2RR performance of the 3D CTPI catalyst under various CO_2 concentrations. **(A)** Current densities obtained for various CO_2 partial pressures. **(B)** Corresponding H_2 FE. **(C)** Corresponding CO FE. **(D)** Corresponding C_2H_4 FE. **(E)** Peak ethylene EE distribution for various CO_2 partial pressures. Full-cell potentials are presented without iR compensation. Operating conditions of the MEA electrolyzer: 0.1 M $KHCO_3$ continuous anolyte was supplied to the anode side with the flow rate of 20 mL min^{-1}; fully humidified CO_2 was supplied to the cathode side with the flow rate of around 80 sccm; and cell temperature was kept constant at around room temperature. The catalyst enables EEs of >20% at partial current densities higher than 120 mA cm^{-2} under the CO_2 concentrations of 10% – 100%. The high EEs obtained even under constrained CO_2 availability highlight the reaction platform's industrial applicability, where the CO_2 is usually in the diluted form.

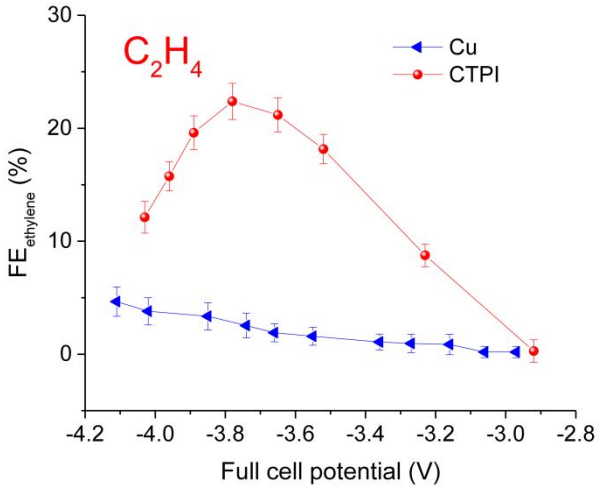

Figure S27. Ethylene FE comparison between reference 3D CTPI and Cu/PTFE towards ethylene electrosynthesis from simulated flue gas. Full-cell potentials are presented without iR compensation.

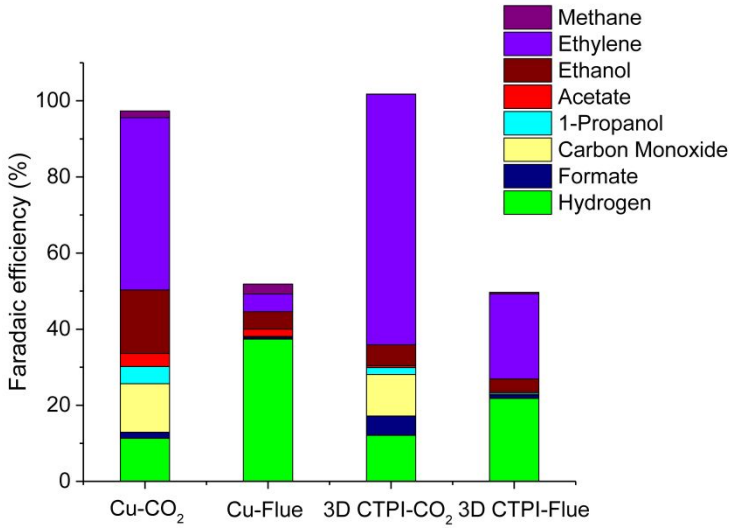

Figure S28. CO_2RR product distribution of the reference Cu/PTFE and 3D CTPI catalyst for either pure CO_2 or simulated flue-gas feeds. The product spectra for pure CO_2 feed were obtained by applying constant current densities that enable the highest ethylene FE towards, which were around 150 mA cm^{-2} and 300 mA cm^{-2} for the Cu/PTFE and 3D CTPI, respectively. Similarly, the product spectra for simulated flue-gas feed were obtained by applying constant current densities that enable the highest ethylene FE , which were around 280 mA cm^{-2} and 320 mA cm^{-2} for the Cu/PTFE and 3D CTPI, respectively. Operating conditions of the MEA electrolyzer: 0.1 M $KHCO_3$ continuous anolyte was supplied to the anode side with the flow rate of 20 mL min^{-1}; fully humidified CO_2 was supplied to the cathode side with the flow rate of around 80 sccm; and cell temperature was kept constant at around room temperature. When simulated flue gas composed of CO_2, CO, O_2, SO_2, and N_2 used as the feedstock, both the Cu/PTFE and 3D CTPI hierarchical reaction platform losses efficiency to the parasitic oxygen reduction reaction (ORR) and hydrogen evaluation reaction (HER). However, 3D CTPI reaction platform – compared to the unmodified Cu/PTFE – provides relatively higher CO_2RR efficiency, a large portion of which is devoted to ethylene.

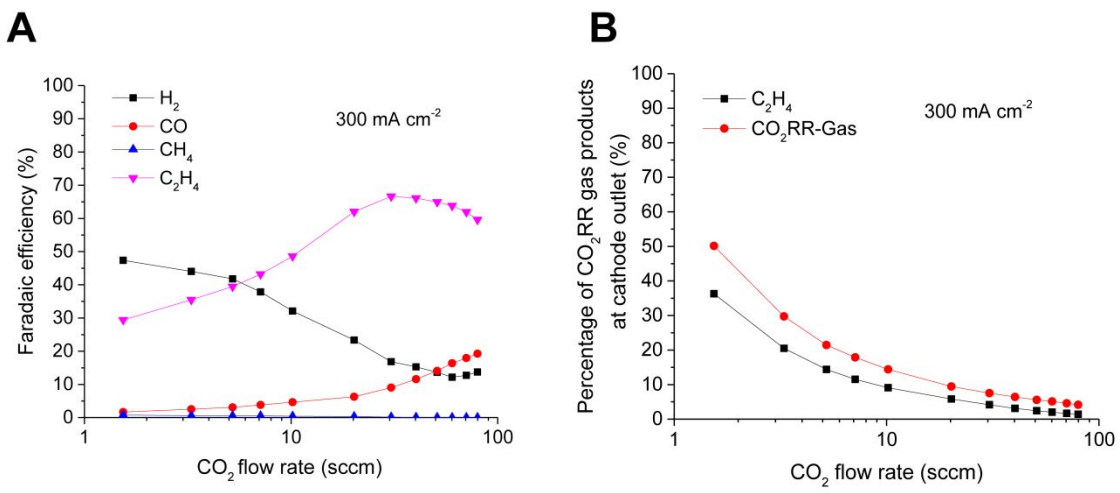

Figure S29. Concentrated ethylene production enabled by 3D CTPI catalyst in the MEA electrolyzer. (A) Effect of CO_2 flow rate on the selectivities of CO_2RR gas products at a constant current density of 300 mA cm^{-2}. **(B)** Ethylene composition at the cathode outlet relative to overall CO_2RR gas products as a function of CO_2 flow rate. Operating conditions of the MEA electrolyzer: 0.1 M $KHCO_3$ continuous anolyte was supplied to the anode side with the flow rate of 20 mL min^{-1}; fully humidified CO_2 was supplied to the cathode side with the various flow rates in the range of 80 – 3 sccm; and cell temperature was kept constant at around room temperature. Obtaining concentrated gas products at the cathode outlet offers a route to decrease the gas product separation costs[2]. We gradually decreased the flow rate of CO_2 supplied to the MEA electrolyzer at the constant current density of 300 mA/cm^2, beginning from 85 to 3 sccm, with fairly small flow rate decrements. The CO_2-to-ethylene conversion becomes more selective at intermediate flow rates, achieving the plateau at around 30 sccm. The increasing ethylene selectivity can be ascribed to a relatively higher local pH built at the reaction region. The increased pH in turn is likely to arise from comparatively mild reaction between CO_2 and hydroxide ions and/or desirable coverage of reaction intermediates on catalyst surface[2]. However, lowering the CO_2 flow rate reduces the availability of CO_2 at the electrochemically active sites,

and hence favoring competing hydrogen evaluation reduction (HER) reaction. The ethylene concentration at the cathode demonstrates a parabolic increase with lowering CO_2 flow rate, achieving the plateau of 37% at the lowest achievable CO_2 inlet flow rate of 3 sccm. The maximum CO_2RR gas product concentration at the cathode outlet reaches its plateau of 50.1% for the inlet CO_2 flow rate of 3 sccm. These findings indicate that the developed MEA electrolyzer can sustain high selectivity towards CO_2RR gas products even at limited CO_2 availability, and hence provide ethylene composition of 37% at the cathode outlet.

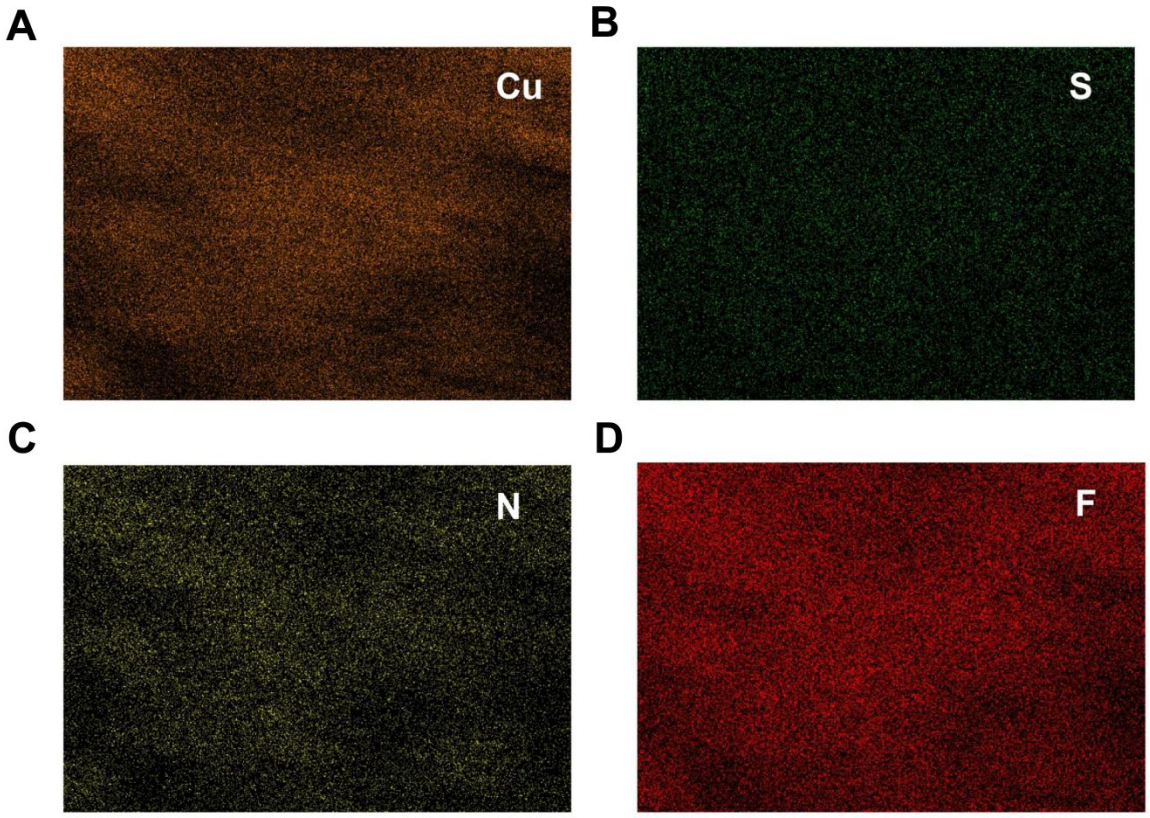

Figure S30. Energy-dispersive X-ray spectroscopy (EDS) of the 3D CTPI catalyst upon completion of a 100-h continuous electrolysis in the MEA electrolyzer. (A) Cu. **(B)** S. **(C)** N. **(D)** F.

References

1. Thevenon, A., Rosas-Hernández, A., Peters, J. C. & Agapie, T. In-situ nanostructuring and stabilization of polycrystalline copper by an organic salt additive promotes electrocatalytic CO_2 reduction to ethylene. *Angew. Chem. Int. Ed.* **2019,** *58,* 16952-16958.
2. Gabardo, C. M. *et al.* Continuous carbon dioxide electroreduction to concentrated multi-carbon products using a membrane electrode assembly. *Joule* **2019,** *3,* 2777-2791.